THE ROLE OF ENDOYTOSIS ON SR-BI MEDIATED LIPID UPTAKE FROM LIPOPROTEINS

THE ROLE OF ENDOYTOSIS ON SR-BI MEDIATED LIPID UPTAKE FROM LIPOPROTEINS

By

AYESHA MUSHEER AHMED, B.Sc.

A Thesis

Submitted to the School of Graduate studies

In Partial fulfillment of the Requirements

For the Degree of Masters of Science

McMaster University

Master of Science (2004)
(Biochemistry and biomedical Sciences)

MCMASTER UNIVERSITY
Hamilton, Ontario

TITLE: The Role of Endocytosis in SR-BI Mediated Lipid Uptake from Lipoproteins

AUTHOR: Ayesha Musheer Ahmed, B.Sc.

SUPERVISOR: Dr. Bernardo L. Trigatti

Number of Pages: xii ,93

Abstract

Scavenger receptor Class B type I (SR-BI), is a multiligand cell surface receptor with broad binding specificity. It is an atypical member of the scavenger receptor family of cell surface receptors, due to its unique binding properties. SR-BI is mostly studied in the context of cholesterol metabolism, as its ligands include lipoproteins, which are the primary vesicles of cholesterol trafficking in the body. Lipoprotein ligands of SR-BI include chemically modified lipoproteins which are associated with retention and accumulation of lipids in the body (leading to disease conditions), as well as unmodified lipoproteins which are involved in clearance of cholesterol from the body and maintenance of normal homeostasis. SR-BI is the only known physiologically relevant receptor of high density lipoprotein particle (HDL), and has been shown to play an important role in HDL metabolism. The mechanism of SR-BI mediated transfer of lipid from lipoprotein has not yet been elucidated. However, several studies have proposed the involvement of known mechanisms of endocytosis in SR-BI mediated transfer of lipids from HDL. Given the broad spectrum of ligands that bind SR-BI and the high specificity of binding and uptake of ligands, we propose that the SR-BI mediates uptake of lipoproteins in a ligand dependent manner. Using lipoprotein ligands labelled with a fluorescent lipid we demonstrated that blocking cellular endocytosis by potassium depletion, hyperosmolarity and disrupting the structure of microfilaments in cells, has a differential effect on murine SR-BI mediated lipid transfer from modified lipoprotein (Ac-LDL) and native lipoprotein (HDL.) Lipid transfer from Ac-LDL is susceptible to these treatments, whereas lipid transfer from HDL was not affected to the same extent.

On the other hand, human SR-BI mediated lipid transfer from both Ac-LDL as well as HDL is affected under these conditions. However, human SR-BI was shown not to co-localize with clathrin, in the presence of HDL and Ac-LDL, dismissing the possibility that clathrin mediated uptake might be involved in lipid uptake by cells. Using a dominant negative mutant of dynamin 1 (Dyn1-K44A) we showed that murine and human SR-BI mediated lipid uptake from HDL and AcLDL is dynamin dependent. Using stable cell lines expressing fluorescent protein tagged human SR-BI, and fluorescent lipid tagged HDL and Ac-LDL, we were able to show the dynamics of human SR-BI mediated lipid uptake in cells. This process was shown to be dependent on microfilament and microtubules.

ACKNOWLEDGMENTS

I would like to thank my supervisor Dr. Dino Trigatti for his guidance and support. He is credited for creating a motivating and stimulating lab environment, conducive for learning and passing on knowledge. I would like to acknowledge the help and guidance I received from my committee members, Dr. Juliet Daniels and Dr. Ray Truant. It was a pleasure working with all the members of the Trigatti lab past and present; I would like to acknowledge the help of Dr. Scott Covey. During my studies at McMaster I have had the privilege of being in the company of friends who did not 'let school interfere with my education' (Mark Twain), for that I am grateful to Lisa Fu, Aneesa Rahaman, Matthew Bates, Ali Rizvi, Tom Baumgartner, Kevin Cheung, Rachelle Brunet and Shane Turcott for enhancing this learning experience and challenging me to think outside the box. I would like to acknowledge the support, kindness and generosity of my family Salman Ali, Fatima Ahmed, Maryam Ahmed, Hasan Ahmed and Umar Ahmed, who keep me motivated and grounded. Most of all I am grateful to my parents Col. (retd) Musheer Ahmed and Anjum Ahmed, who have always been committed to supporting all my endeavors. Their unwavering faith, sacrifice and encouragement is instrumental in my every success.

Table of Contents

List of Figures

List of tables

List of Abbreviations

AcLDL	**Acetylated Low Density Lipoprotein**
ApoB	**Apolipoprotein B**
FACS	**Fluorescence Activated Cell Sorting**
HDL	**High Density Lipoprotein**
hSR-BI	**Human Scavenger Receptor Class B Type I**
LDL	**Low Density Lipoprotein**
mSR-A1	**Murine Scavenger Receptor Class A Type I**
mSR-BI	**Murine Scavenger Receptor Class B Type I**
oxLDL	**Oxidized Low Density Lipoprotein**
SR-BI	**Scavenger Receptor Class B Type I**
VLDL	**Very Low Density Lipoprotein**

1. Introduction:

1.1. Scavenger receptors and lipoprotein ligands

Scavenger receptors are a class of cell surface receptors, which are defined by their ability to bind and mediate the uptake of a variety of ligands. These multiligand receptors were initially identified by Brown and Goldstein as receptors that can bind chemically modified lipoprotein such as oxidized low density lipoprotein (oxLDL) and acetylated low density lipoprotein (Ac-LDL) (Brown et al., 1979). They discovered that acetylation of the apolipoproteins on the low density lipoprotein (LDL) particles results in the uptake of cholesterol by novel pathways, other than the classic LDL receptor, in macrophages. Later Brown and Goldstein showed that these novel receptors can mediate the binding of many other ligands (including modified proteins, sulphate polysaccharides and certain polynucleotides). Due to their broad binding specificity these receptors were named macrophage "scavenger receptors". The first scavenger receptor to be cloned was the bovine scavenger receptor Class A type I (bSR-AI) (Kodama et al., 1990). Since then, cDNAs of many other scavenger receptors have been cloned from a variety of cell lines. These receptors have been categorized into broad classes based on sequence and structural similarities (Krieger et al., 1994). The focus of my study is a member of class B of scavenger receptors called scavenger receptor class B type I (SR-BI).

1.2. Scavenger receptor class B type I

SR-BI is a 509 amino acid long integral membrane protein. It was first identified as a scavenger receptor by an expression cloning study using Ac-LDL as a ligand (Acton et al., 1994). SR-BI was shown to have 30 percent sequence identity with CD36 (Calvo et al., 1997) protein, a previously identified class B scavenger receptor. It has been proposed that SR-BI has two transmembrane regions that anchor the receptor on the cell membrane. The amino and carboxyl termini were predicted to be inside the cell, while the rest of the protein was predicted to be exposed outwards to the extracellular region (Figure 1). The predicted molecular weight for SR-BI is 57 kDa, but it migrates with an apparent molecular weight of 84 k Da, upon denaturing electrophoresis (Babitt et al., 1997). This shift in apparent molecular weight is attributed to N-glycosylation on eleven proposed sites (Babitt et al., 1997). SR-BI is also fatty acylated on two carboxyl terminal cysteines (Babitt et al., 1997).

1.3. Ligands of SR-BI

SR-BI has been shown to bind most of the ligands typically associated with scavenger receptors, including modified proteins such as maleylated bovine serum albumin (maleyl-BSA) (Acton et al., 1994); advanced glycosylation end products (AGE modified BSA) (Ohgami et al., 2001); liposomes containing anionic phospholipids (Rigotti et al., 1995); apoptotic cells; and modified lipoproteins such as acetylated LDL (Ac-LDL) (Murao et al., 1997), oxidized LDL (Calvo et al., 1997; Murao et al., 1997) and oxidized HDL (Marsche et al., 2002). However unlike other scavenger receptors, SR-

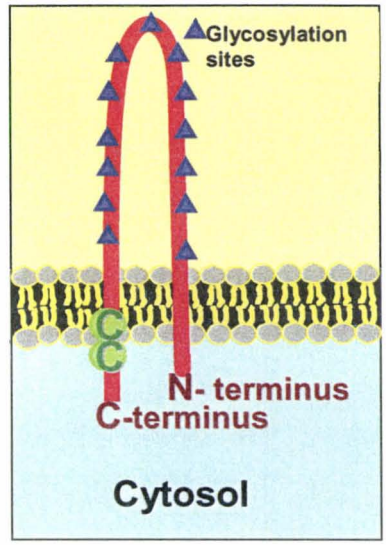

Figure 1. Schematic illustration of SR-BI topology. SR-BI is an integral membrane protein, spanning the cell membrane. The amino and slightly longer carboxyl tail of the protein are proposed to be inside the membrane while the bulk of the protein is exposed to the extra cellular space. SR-BI is palmitoylated on two cysteine residues and has 11 proposed glycosylation sites.

BI does not bind several polyanions (fucoidin, carrageenan, and polyguanosinic acid) that are established ligands of class A scavenger receptors (Acton et al., 1994).

In contrast to other classes of scavenger receptors, SR-BI was shown to bind unmodified lipoproteins such as very low density lipoprotein (VLDL) (Calvo et al., 1997), low density lipoprotein (LDL) (Acton et al., 1994) and high density lipoprotein (HDL) (Acton et al., 1996). LDL receptor had been established as the physiological receptor for LDL well before the discovery of SR-BI. The relatively high affinity of SR-BI for HDL (dissociation constant of 30μg/ml) (Acton et al., 1996) raised the possibility that SR-BI could be the long sought after physiological receptor for HDL.

1.4. Lipoprotein ligands of SR-BI have diverse physiological functions

1.4.1. Lipoproteins

SR-BI has been studied mostly in the context of cholesterol and lipid metabolism. Lipids are hydrophobic molecules, insoluble in the aqueous environment of the body. In order to be transported in the blood, esterified cholesterol and other lipids are packaged into lipoprotein particles. Lipoproteins consist of a hydrophobic core of triglycerides and cholesterol esters, surrounded by a polar monolayer of phopospholipids and free cholesterol that enable the transport of lipids in blood. Lipoproteins also have protein constituents called apolipoproteins that are associated with the phospholipid monolayer. Lipoproteins are classified based on their relative buoyant density, determined by the ratio of protein to lipid. The nomenclature for lipoproteins identifies and distinguishes them based on their relative densities. For example, 'very low density lipoprotein,' 'low

density lipoprotein' and 'high density lipoprotein' have increasingly higher buoyant densities and therefore increasing protein to lipid ratios. Lipoproteins also vary in their apolipoprotein constituents. For example, apolipoprotein apo B is the apolipoprotein constituent of LDL, but HDL contains a variety of apolipoproteins, the major constituent being apo A1. Figure 2 shows a schematic diagram of LDL and HDL, which are the two most abundant lipoproteins in the plasma.

1.4.2. Functions of native and chemically modified lipoproteins

Lipoproteins are subject to chemical modifications on the lipid and apolipoprotein components, such as acetylation and oxidation. Chemically modified lipoproteins have very different physiological roles in cholesterol metabolism than unmodified lipoproteins. Modified lipoproteins are associated with disease conditions, while the levels of unmodified lipoproteins are correlated with protection against disease (Krieger, 2001). For example, modification of apolipoprotein on lipoprotein particles have been shown to promote atherosclerosis. LDL and VLDL are retained in the artery wall and undergo a variety of modifications (proteolytic digestion, oxidation, aggregation). These modified lipoproteins are taken up by macrophages and possibly other cells and contribute to the formation and accumulation of lipid in cells, leading to the formation of lipid engorged cells, called foam cells (de Winther et al., 1999). Foam cells are thought to be involved in early stages of formation of an atherosclerotic plaque in the artery wall (de Villiers et al., 1999). These plaques gradually build up and reduce blood flow (atherosclerosis) contributing to the development of coronary heart disease and stroke. If blockage occurs,

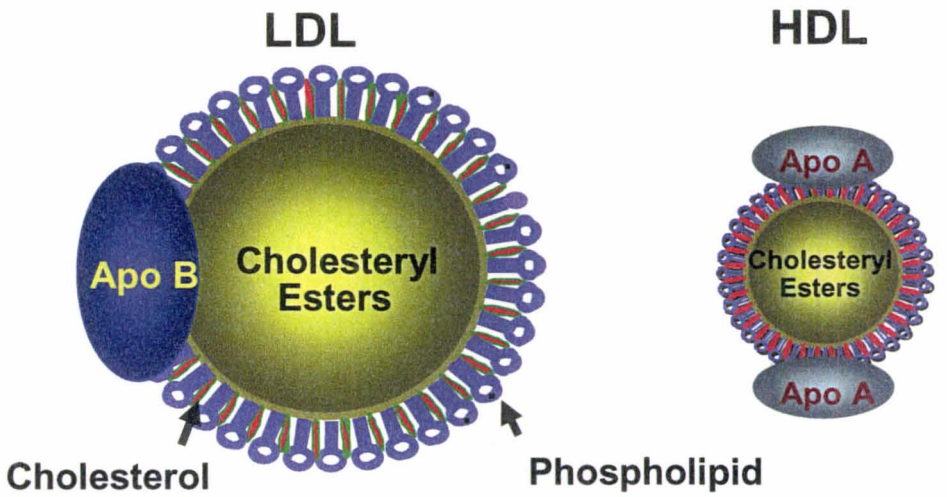

Figure 2. Schematic illustration of the salient structural features of lipoprotein particles. Lipoproteins are composed of a hydrophobic core of lipids, cholesterol esters and triglycerides. The surface of lipoprotein is composed of a monolayer of polar phospholipids and free cholesterol. They are classified based on their buoyant density. LDL has a low buoyant density than HDL due to its larger lipid to protein ratio. The protein constituents of lipoproteins are called apolipoproteins. Major apolipoprotein on LDL is apolipoprotein B whereas the major lipoprotein on HDL is apolipoprotein A.

caused by either the gradual formation of plaques or the rapid formation of a blood clot, the result is a heart attack or a stroke. Incubation of macrophages and smooth muscle cells with modified lipoproteins such as Ac-LDL has been shown to result in the accumulation of cytoplasmic lipid droplets and the conversion of cells to foam cells *in vitro* (cell culture) (de Villiers and Smart, 1999). In contrast, high levels of unmodified HDL in plasma is correlated with protection against atherosclerosis, possibly due to its involvement in cholesterol clearance from peripheral tissues like macrophages by 'reverse cholesterol transport' (Gu et al., 2000[a]). The ability of SR-BI to bind and mediate transfer from both modified as well as native lipoproteins makes it a unique receptor, as it is able to mediate the lipid uptake from lipoproteins which play different physiological roles in disease conditions in the same cell type (such as the macrophage).

1.4.3. Physiological role of SR-BI in HDL metabolism

HDL plays a role in 'reverse cholesterol transport', a process by which it takes up excess cholesterol from peripheral cells (like macrophages in artery walls) and transports it to the liver, where it is secreted into bile or repackaged into nascent lipoproteins and secreted into plasma (Trigatti et al., 2000). Studies in transgenic mice have established that SR-BI has a significant role in HDL metabolism *in vivo*. Mice with hepatic over-expression of SR-BI, were reported to have an increase in cholesterol secretion in bile, with no change in other components of bile, such as bile acid, and a decrease in HDL cholesterol in plasma (Kozarsky et al., 1997). On the other hand, in SR-BI knock out mice, there was reported to be an increase in plasma HDL cholesterol, a reduction in

cholesteryl ester clearance and as well as a decrease in biliary cholesterol level (Rigotti et al., 1997). These studies established hepatic SR-BI as an important receptor mediating reverse cholesterol transport from HDL. SR-BI was also shown to be expressed abundantly in tissues other than liver that are involved in cholesterol metabolism, such as macrophages and steroidogenic tissues (Calvo et al., 1993; Murao et al., 1997). In steroidogenic tissues cholesterol is taken up and stored for steroid hormone synthesis. SR-BI knock out mice were reported to be unable to store cholesterol in steroidogenic tissues (such as adrenal gland and ovaries) (Trigatti et al. 1999; Krieger et al. 2001). This finding further established SR-BI as an important physiological receptor in HDL metabolism.

1.5. Mechanism of SR-BI mediated transfer of lipid from lipoproteins

1.5.1. LDL receptor mediated lipid uptake from LDL

LDL receptor mediated lipid transfer is the major route of cholesterol transport in the body. The mechanism of LDL receptor mediated uptake of lipid from LDL particle is well understood. LDL was shown to be internalized in cells by LDL receptor mediated endocytosis via clathrin coated pits (Figure 3). Binding of the LDL to LDL receptor results in a clustering of receptor-ligand complexes on the membrane, mediated by an adaptor protein called AP-2. Adaptor proteins interact with plasma membrane phospholipids and cytoplasmic domains of receptors. When adaptor proteins are bound to the plasma membrane, they recruit a structural protein called 'clathrin' to the cell membrane (Ricotta et al., 2002). Clathrin is a protein made up of three clathrin heavy

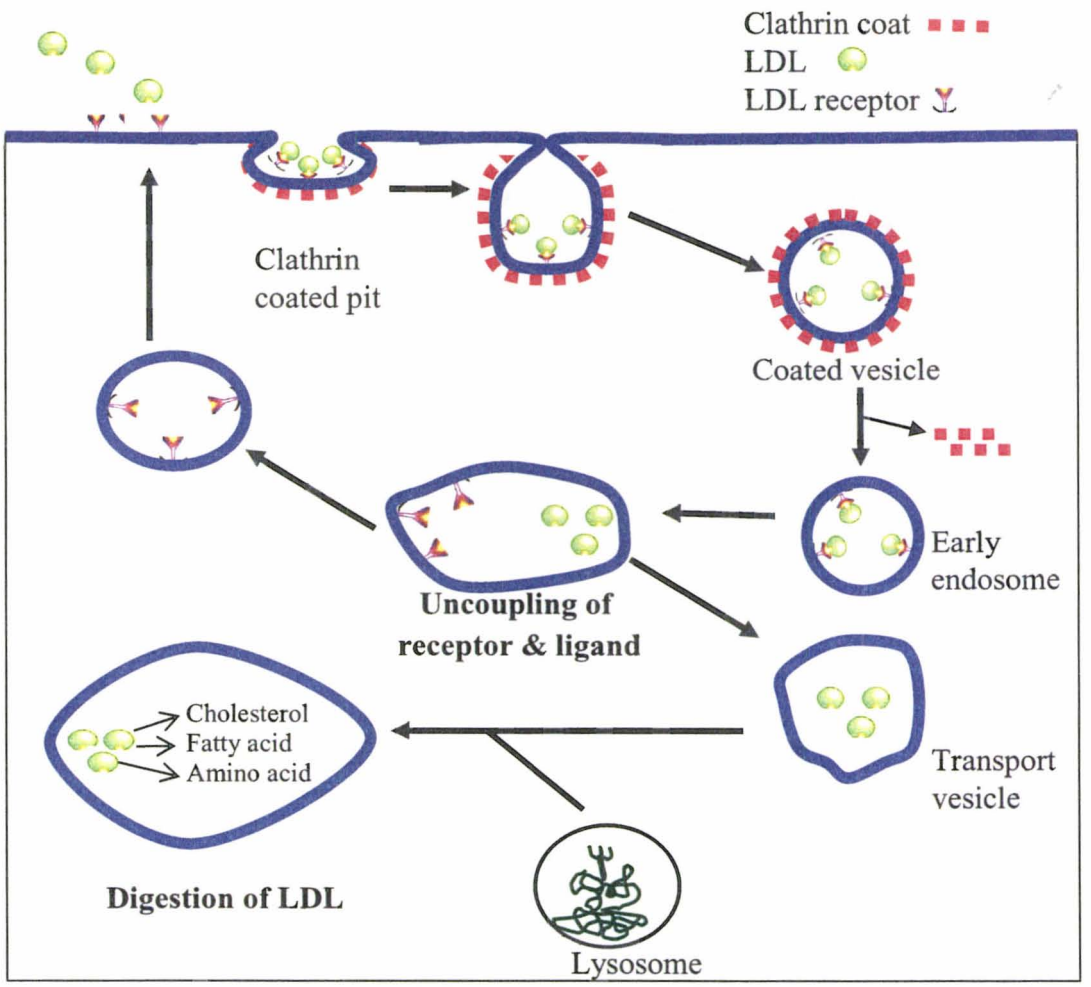

Figure 3. Schematic illustration of the main events in LDL receptor mediated endocytosis of LDL particle via clathrin coated pits. LDL receptor binding to LDL particles leads to receptor clustering into the clathrin coated pits. Clathrin coated pits are internalized into clathrin coated vesicles. Once internalized, clathrin coat disassembles, and the endocytic vesicle is referred to as early endosome. The pH in the early endosome decreases, leading to the uncoupling of the receptor and ligand complex. LDL receptor is carried to the cell membrane, whereas LDL particles are fused with lysosomes. Due to the action of lysosomal enzymes LDL is digested into its constituents (cholesterol, fatty acids and amino acids) which become available to be utilized by the cell.

chains and three clathrin light chains that assemble to form a three-legged structure called a clathrin triskelion (Kirchhausen et al., 1981; Ungewickell et al., 1981). Clathrin triskelion forms the 'clathrin lattice' that lines the inner surface of plasma membrane. 'Clathrin coated' membrane forms invagination in the membrane, called 'clathrin coated pits.' LDL receptor- ligand complex localized in clathrin coated pits which are pinched off the membrane and internalized as 'clathrin coated vesicles.' A family of GTPases called Dynamin is involved in the fission of clathrin coated pits from the membrane (Sever et al., 2000). Once internalized, clathrin coated vesicles shed their clathrin coats, and are known as early endosomes. The internal pH of early endosomes lowers to pH 5, resulting in a conformational change in the LDL receptor (Beglova, 2004), causing the dissociation of LDL. LDL receptors are recycled back to the plasma membrane and LDL particles are transported to the lysosome where hydrolysis occurs. The components of LDL (cholesterol, lipids and amino acids) thus become available to be utilized by the cell (Brown et al., 1986). Receptor-mediated endocytosis via clathrin coated pits was later found to be the involved in receptor-mediated uptake by several cell surface receptors, such as transferrin receptor that mediates the internalization of transferrin (iron binding protein) receptor.

1.5.2. SR-BI mediated selective uptake of lipid from lipoprotein:

Unlike LDL, SR-BI was proposed to mediate the uptake of lipid components of HDL (cholesterol esters, phospholipids and triglycerides), without the *net* internalization or degradation of HDL particles in the liver (Acton et al., 1996). This process is termed

SR-BI mediated 'selective uptake'(Acton et al., 1996). Evidence for SR-BI mediated selective uptake came from studies using lipoproteins labeled with ^{3}H-cholesterol esters and ^{125}I-labelled apolipoproteins tracers, in cultured cells expressing *murine* SR-BI. These studies showed that cells incubated in media containing double labeled lipoproteins take up tritiated cholesterol (determined by an accumulation of tritium), without the corresponding depletion of ^{125}I-labelled lipoprotein particles from the incubation medium (Acton et al., 1996). ^{125}I-labelled lipoprotein particles were found to be depleted in their cholesterol ester component (Ji Y *et al.* 1999), suggesting a selective uptake of cholesterol esters from the lipoprotein particles. Figure 4 illustrated the process by which SR-BI was thought to mediate selective uptake on the cellular level. HDL particles enriched with cholesterol esters bind SR-BI on cell surface. Cholesterol esters are selectively internalized followed by the release of cholesterol ester depleted HDL particles. Similar studies have shown SR-BI mediated selective uptake of lipids, using lipoproteins labeled with fluorescent lipids (such as DiI) and alexa-488 labeled apolipoproteins (Acton et al., 1996). SR-BI has also been shown to mediate selective up take from LDL, to a much lesser extent (Stangl et al., 1999).

In addition to mediating influx of lipid, SR-BI has also been proposed to mediate the efflux of cholesterol from cells to HDL particles (Krieger, 2001). It has been noted that the selective uptake and efflux to HDL and LDL decreases considerably in mutant SR-BI molecules unable to bind these lipoproteins; indicating that binding to the receptor is important for SR-BI mediated selective uptake and efflux to take place (Gu et al., 2000[a]; Rigotti et al., 1997). It was shown that expression of SR-BI in bone marrow

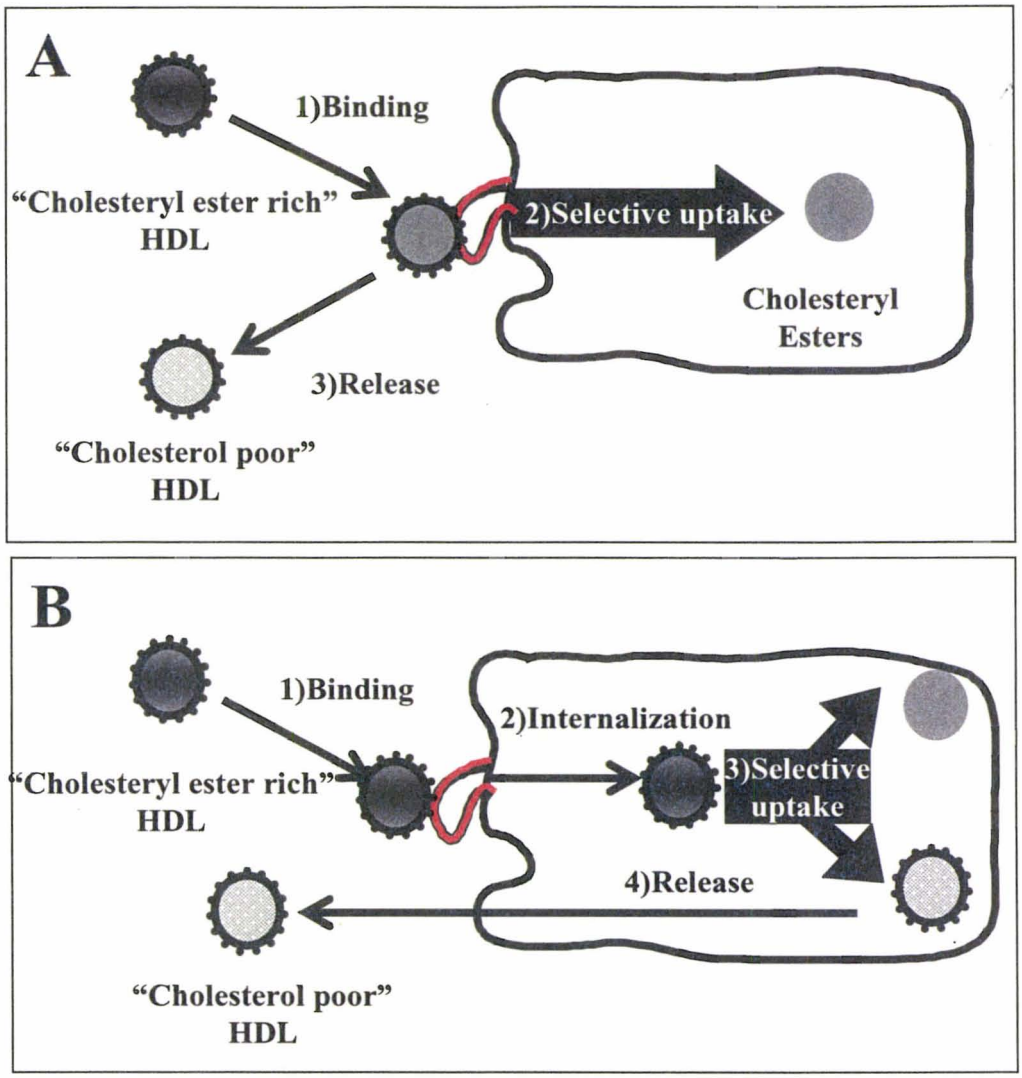

Figure 4. Illustration of proposed models of SR-BI mediated selective uptake of cholesterol from HDL, on the cellular level. HDL containing cholesteryl ester 'cholesteryl ester rich,' binds SR-BI on cell surface. Binding is followed by the selective uptake of cholesterol esters, from the lipoproteins into the cell (A) or internalization of lipoprotein and selective uptake of cholesterol esters within the cells (B). In both models 'Cholesterol poor' HDL is released from the cell, without being degraded like the LDL particle in the LDL receptor pathway.

derived cells (such as macrophages) contributes to this protection against atherosclerosis (Covey et al., 2003).

1.5.3. SR-BI has specific binding sites for multiple ligands

Although, the overall mechanism of SR-BI mediated selective uptake from lipoproteins is not known, several specific residues in the extra cellular domain of SR-BI have been identified as being important for its interaction with lipoprotein, and selective uptake of lipid. Studies reveal that SR-BI has distinct binding sites and modes of binding different lipoproteins. For instance, point mutations in the SR-BI sequence (Gln 401Arg, Gln402Arg, Gln418Arg) were shown to affect HDL binding, but these mutations had no effect on LDL binding (Gu et al., 2000[a]). Another mutation (Met158Arg) was shown to abolish SR-BI binding of HDL as well as LDL, but had no effect on SR-BI binding of Ac-LDL (Gu et al., 2000[a]).

SR-BI was shown to bind both LDL and HDL with high affinity. SR-BI has a higher binding affinity for LDL (dissociation constant of 10 μg/ml) (Acton, 1994) than HDL (dissociation constant of 30 μg/ml) (Acton et al., 1996), but it has been shown to preferentially bind HDL over LDL. Evidence for this finding came from binding studies using LDL and HDL, which showed that LDL competes poorly with HDL for SR-BI receptor binding; this phenomenon is termed 'non reciprocal cross competition'(Krieger and Herz, 1994).

1.6. Proposed mechanisms of SR-BI mediated lipid transfer from HDL

The endocytic pathway utilized by the LDL receptor does not seem to fit the model of 'selective uptake' by SR-BI. However, there is some indirect evidence that points towards the involvement of endocytosis in SR-BI mediated lipid transfer from lipoproteins. This evidence comes from incubation of cells expressing *murine* SR-BI, with alexa 488 labeled HDL. Alexa-488 was used to label the HDL particles' on the non-exchangeable protein components (apolipoproteins). At 4°C alexa 488-HDL was shown to bind and remain bound to the cell surface, which upon incubation at 37°C (temperature which is permissive for endocytosis) subsequently moved into the cells and co-localize with transferrin containing compartments (Silver et al., 2001[b]). Transferrin is known to be endocytosed via clathrin mediated pathway, but unlike LDL particles, it is not sorted to the lysosomal degradation pathway; instead it is recycled back to the cell surface (Iacopetta et al., 1983). Localization of alexa-HDL within transferrin containing compartment suggests that after binding to SR-BI, HDL is transiently internalized and then re-secreted back to the cell surface and released into the extra-cellular space (much like transferrin). This idea of transient internalization is consistent with SR-BI mediated selective uptake and suggests that HDL may be relieved of its lipid cargo inside an endocytic compartment (Silver et al., 2001[b]). SR-BI itself has also been shown to co-localize with transferrin in endocytic compartments (Silver et al., 2001[b]). In the same study, HDL labeled with alexa-488 as well as a fluorescent lipid tracer (DiI) was shown to transverse polarized liver and kidney cells from the basolateral membrane to the apical membrane, via endocytic recycling compartments, again suggesting transient

internalization of HDL. However, this study did not establish whether the internalization of HDL is a necessary step in the overall process of SR-BI mediated lipid transfer from HDL. Moreover, HDL in this study was chemically modified by alexa 488-labeling of the apolipoproteins. As mentioned before, chemical modifications of apolipoproteins (such as oxidation and acetylation) have previously shown to alter their SR-BI binding properties. Therefore, alexa488-HDL may not be a suitable marker for native HDL.

Colocalization of SR-BI and HDL with transferrin alludes to the involvement of clathrin mediated endocytosis in SR-BI mediated lipid transfer from HDL. But to date, there has been no direct evidence to link SR-BI mediated uptake of lipid with clathrin mediated endocytosis. SR-BI was shown not to co-localize with clathrin-coated pits in the cells (Babitt et al., 1997). However, it was shown by fractionation of plasma membrane that *murine* SR-BI co-fractionates with caveolin-1 protein. Co-localization studies using immunofluorescence microscopy confirms that *murine* SR-BI co-localizes with caveolin-1 in a punctate pattern across the surface and on the edge of cells (Babitt et al., 1997). Caveolin-1 is a constituent protein of microdomains called caveolae.

Caveolae are plasma membrane domains rich in cholesterol and sphingomyelin. Caveolae are defined morphologically, as flask-shaped invaginations in the plasma membrane. They are characterized by a filamentous coat consisting of caveolin proteins on the inside surface of caveolar membrane (Nabi et al., 2003). Caveolae are the sites of cholesterol uptake in the cells, they are also involved in signal transduction and the intracellular transportation of other lipid raft-associated molecules (Parton RG, 1994). Caveolae have endocytic functions that differ from the clathrin-coated pit pathway.

Potocytosis is a term used by some to describe a mechanism by which small and large molecules as well as macromolecular complexes are sequestered and transported by caveolae (Anderson et al., 1992; Nabi and Le, 2003.; Parton RG, 1994; RG Parton, 1994). Several macromolecules including folic acid, bacterial toxins including cholera toxin, and some viruses including SV40, make use of caveolar endocytosis to enter cells. Partial co-localization of SR-BI with caveolae raises the possibility that the unique properties of these specialized cell surface domains may play a critical role in SR-BI mediated transfer of lipids between lipoproteins and cells (Babitt et al., 1997). The role of caveolae mediated endocytosis in cellular uptake of lipid from lipoprotein remains to be explored.

There have been two studies that suggested that SR-BI mediated lipid transfer from HDL does not involve any cellular pathway. One group of researchers used purified SR-BI reconstituted into phosphatidylcholine / cholesterol liposomes to show that SR-BI mediates lipoprotein binding and selective lipid transfer (Liu et al., 2002). This suggests that both SR-BI-mediated HDL binding and selective lipid uptake are intrinsic properties of the receptor, and they are not dependent on other proteins or specific cellular structures or compartments. Another group of researchers have suggested that SR-BI mediates lipid transfer by providing a hydrophobic channel allowing lipid transfer by diffusion from the lipoprotein particle to the plasma membrane (Rodrigueza et al., 1999). However, these studies did not adequately address the physiological relevance of the mechanisms shown to be involved in SR-BI mediated lipid transfer.

In other words, it may be that in a cell free system SR-BI is able to transfer a portion of lipid form HDL autonomously. But there is no indication as to what is the contribution of this process to the over all process of SR-BI mediated lipid uptake in cells. At lease two cellular proteins have been shown to be indirectly involved in SR-BI mediated lipid transfer. Binding of SR-BI to CLAMP protein is essential for its expression on cell surface (Ikemoto et al., 2002) and caveolin-1 has been shown to be a negative regulator of SR-BI mediated cholesterol ester transfer . But whether or not the presence of SR-BI is sufficient in mediating transfer of lipid from HDL without the involvement of cellular machinery is yet to be determined using cell based assays.

1.7. Investigating the role of endocytosis in SR-BI mediated lipoprotein transfer

We were interested in characterizing the physiologically relevant mechanism by which SR-BI mediates lipid transfer from lipoprotein ligands into the cell. The focus of my project was to determine whether SR-BI mediated endocytosis of lipoproteins is necessary for SR-BI mediated transfer of lipid from lipoproteins into the cell. Based on the fact that SR-BI binds a variety of ligands, that have diverse physiological function and that SR-BI has specific and distinct binding sites for different lipoprotein ligands; we explored the possibility that SR-BI mediated lipid transfer may follow several different pathways, depending on the lipoprotein ligands. Our approach was to test the involvement of endocytosis in SR-BI mediated lipid transfer from modified lipoproteins and unmodified lipoproteins simultaneously.

1.7.1. Known endocytosis pathways in cells

To date, several different mechanisms of endocytosis have been illustrated in mammalian cells. These pathways include clathrin-mediated, caveolae mediated, clathrin and caveolae independent endocytosis, fluid-phase endocytosis and phagocytosis. These pathways differ with regards to the nature of internalized cargo, the size of vesicles, molecular machinery involved, and the type of regulation. Clathrin mediated endocytosis is the best characterized of the endocytic pathways. Based on structural studies, clathrin-mediated endocytosis in mammals has been subdivided into distinct stages: clathrin coat assembly on membranes, vesicle invagination, fission, movement of vesicles into the cell interior, vesicle uncoating, and fusion with early endosomes. These steps have been illustrated for LDL receptor mediated uptake of LDL particle in section 1.4.1.

Caveolae mediated endocytosis is characterized by its clathrin independence. Caveolae are characterized by their morphological appearance (see above) and association with caveolin proteins. Caveolae are implicated in the endocytosis of extra cellular ligands such as folic acid, bacterial toxins including tetanus and cholera, as well as uncoated polyoma or simian virus (SV40) (Nichols, 2003). Compared to clathrin-dependent endocytosis, little is known about different stages of caveolae formation. Dynamin proteins and actin filaments are implicated in the ligand stimulated internalization of (otherwise static) cavolae from the plasma membrane (Pelkmans et al., 2002). Once internalized, markers of caveolae (ligands such as SV40 or cholera toxin subunit B) were detected in a structure resembling an early endosome, called caveosome by some (Nabi and Le, 2003; Pelkmans and Helenius, 2002). Caveosomes lack protein markers typically associated with classical early endosome involved in clathrin mediated

endocytic pathway; unlike classical endosomes caveosomes were shown to have a neutral pH environment. Caveosomes have been shown to be involved in transcytosis and delivery of ligands to endoplasmic reticulum (Nabi and Le, 2003). Microtubules are shown to be involved in intracellular movement of caveosomes in cells.

Pinocytosis is the process by which cells take up extracellular fluid. Pinosomes are large vesicles (0.5–5 μm in diameter) that internalize extracellular fluid (Swansona et al., 1995). The process of phagocytosis is involved in uptake of solid particles (>200nm) by specialized cells such as macrophages and dendritic cells (Swansona and Watts, 1995; Cardelli, 2001). In addition to these, some ligands have been shown to be taken up by other endocytic pathways not involving clathrin coated pits or caveolae. Although these pathways are poorly characterized, they are implicated in endocytosis of some viruses, toxins and interleukin-2 receptor (Subtil et al., 1994).

Clathrin mediated, caveolae mediated and clathrin and caveolae independent endocytic pathways are distinct from each other. However, some elements of cellular machinery have been shown to be involved in all endocytic pathways. For example, microfilaments, components of cytoskeleton constituted of actin polymers are implicated in the internalization of endocytic vesicles (Apodaca, 2001; Qualmann et al., 2000). Microtubules, the other component of cytoskeleton made of tubulin polymers has been shown to participate in trafficking of endocytic vesicles in cells (Apodaca, 2001; Mundy et al., 2002). The dynamin GTPase family of proteins is believed to be involved in the fission of the all endocytic vesicles from the plasma membrane.

There are several treatments which are known to block cellular endocytosis via clathrin coated pits and caveolae. These treatments include depletion of intracellular potassium and incubation of cells with hyperosmolar solutions. Although these treatments are not specific to inhibiting endocytosis in cells, they have been shown to inhibit receptor mediated internalization via clathrin coated pits by inhibiting the assembly of clathrin and formation of clathrin coated pits (Janet, 1983; Larkin et al., 1983). These treatments were also shown to reduce the number of caveolae on the cell surface (Carpentier et al., 1989). Cells treated with potassium depletion and hyperosmolarity were unable to take up markers of clathrin mediated endocytosis (such as transferrin) (Daukas et al., 1985; Heuser et al., 1989) and caveolae mediated endocytosis, such as gold labeled cholera toxin (measured morphologically) (Carpentier et al., 1989).

1.7.2. Investigating the role of cellular endocytosis in SR-BI mediated lipid uptake form lipoproteins

The objective of my project is to determine if SR-BI mediated lipid transfer from lipoproteins is dependent on endocytic processes in the cell. To that end, we tested if inhibiting cellular endocytosis has an effect on SR-BI mediated lipid transfer from lipoprotein ligands in cells expressing SR-BI. As mentioned above, we also predicted that SR-BI mediated lipid transfer from modified lipoproteins may follow a different mechanism than from unmodified lipoproteins.

We used cell based assays to study SR-BI mediated lipid transfer. Stable cell lines expressing *murine* and *human* SR-BI were used to study SR-BI mediated lipid transfer from lipoproteins into the cells. As ligands for lipid transfer, we used *1)* native HDL, with no chemical modifications on the protein constituents and *2)* acetylated LDL (Ac-LDL), LDL that had been chemically modified by acetylation. Lipoprotein ligands were labeled with a fluorescent lipid (dioctadecyl-3,3,3',3'- tetramethylindocarbocyanine perchlorate ('DiI'; $DiIC_{18}$) which allowed us to quantify the transfer of lipid from lipoprotein to cells. SR-BI mediated uptake of DiI was shown to be similar to the uptake of [3H]-cholesterol ester from lipoproteins, this suggested that DiI accumulation was a suitable marker for lipid uptake from lipoproteins (Acton et al., 1996).

Although potassium depletion and hyperosmolarity are widely used to block endocytosis in cells, these treatments are not specific to inhibiting endocytosis in cells. To confirm the results from these treatments we tested the effect of blocking specific steps involved in the process of endocytosis on SR-BI mediated lipid uptake from lipoproteins. Dynamins - a family of GTPase proteins – are shown to be involved in the internalization of endocytic vesicles from clathrin coated pits (Sever et al., 2000) as well as caveolae (Henley et al., 1998). Figure 5 illustrates the role of dynamin in 'pinching off' of clathrin coated vesicle. A dominant-negative mutant of dynamin 1 in which lysine at position 44 is replaced by alanine (dyn1 K44A) has been shown to inhibit the internalization step in both clathrin mediated as well as caveolae mediated endocytosis in

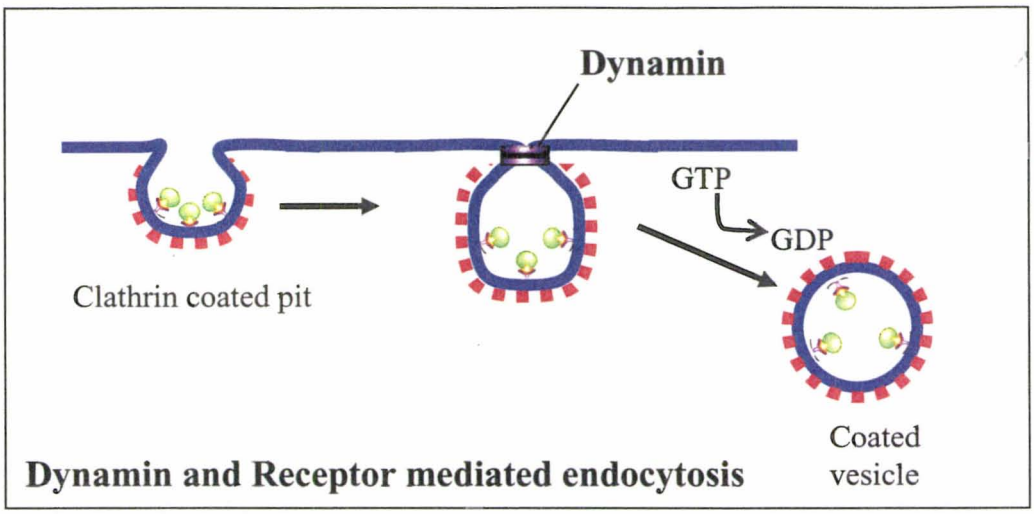

Figure 5. A schematic illustration of Dynamin mediated fission of clathrin coated pits from the cell membrane and internalization as a clathrin coated vesicle. The fission of clathrin coated pits is dependent on the GTPase activity of Dynamins. Dynamin monomers self assemble into tetramers and form 'rings' around the neck of budding vesicles, and through the process of GTP hydrolysis mediate the pinching of the vesicle from the plasma membrane.

cells (Oh et al., 1998). We examined the effect of expressing dyn1 K44A on SR-BI mediated lipid uptake from lipoproteins in cells stably expressing *human* SR-BI or *murine* SR-BI.

We also tested the effect of disrupting microfilaments on SR-BI mediated lipid uptake from lipoproteins. As mentioned above, microfilaments have been shown to play an important role in the internalization of endocytic vesicles from the cell membrane. To test the contribution of endocytosis in SR-BI mediated lipid transfer from lipoproteins, we tested the effect of cytochalasin D, a drug that disrupts endocytosis by disrupting microfilaments (Durrbach et al., 1996; Goddette et al., 1986). We also tested the effect of colchicine, a drug that disrupts movements of endocytic vesicles by disrupting microtubules in cells (Apodaca, 2001; Durrbach et al., 1996; Osland et al., 1979), on SR-BI mediated lipid uptake from lipoproteins in cells. These experiments directly address the role of endocytic processes in the uptake of lipids from lipoproteins by SR-BI. The results also reveal interesting differences in the characteristics of lipid uptake mediated by *murine* SR-BI and *human* SR-BI (also called CLA1).

2. Materials and Method

2.1. **Materials.**

LdlA7 CHOK1, ldlA[*murine* SR-BI] and ldlA[*murine* SR-AI] cells were provided by Dr. Monty Krieger. 495 anti-SR-BI antibody was provided by Dr. Monty Krieger as well. Anti-HA antibody was purchased from Santa Cruz Biotechnology, CA. The alexa 488-goat anti rabbit secondary antibody, cholera toxin B, DiI (C18) and DAPI were purchased from molecular probes. Goat anti rabbit conjugated to HRP and enhanced chemiluminescence reagent was purchased from PerkinElmer Life Sciences (Boston. MA). BCA assay kit was purchased from Pierce (Rockford, IL). X-Omat audioradiography film was purchased from Kodak (Rochester, NY). PVDF membrane was purchased from Millipore (Bedford, PA).

pEGFP-C1, pmRFP-C1, p EYFP-N1 were provided by Dr. Ray Truant (McMaster University, Hamilton). pEGFP-Clathrin and pHA-Dyn1K44A were provided by Dr. Sergio Grinstein. p*human* SR-BI was provided by Dr. Monty Krieger. Primers for PCR were prepared by Mobix lab (McMaster University) or Sigma, Canada. PCR reagents (Taq polymerase and dNTPs were purchased from Promega (Madison, WI). PCR mutagenesis kit was purchased from Stratagene (La Jolla, CA). Tissue culture supplies were purchased from Invitrogen.

Acetone, formaldehyde, glycerol, TritonX-100, ammonium persulfate, ammonium chloride, were purchased from BDH Inc. (Toronto, ON). Aprotinin, bovine serum albumin (fatty acid free), ethylenediaminetetraacetic acid (EDTA), DNAase,

Dimythel sulfoxide (DMSO), isopropanol, leupeptin, 2-mercaptoethanol, paraformaldehyde, poly D lysine, sodium dodecyl sulphate, tetramethylethylenediamine (TEMED) and Tween 20 were purchased from Sigma (St Louis, MO).

2.2 Method

2.2.1 Growth and propagation of cells:

Cells were cultured on 10cm cell culture dishes in 10 ml of medium A (HAM's F12 containing 5 % FBS, 2.0 mM L-glutamine, 50 units/ml penicillin and 50 μg/ml streptomycin) at 37° C in an atmosphere of 5% carbon dioxide. Cells were washed with PBS (warmed to 37°C) and incubated with 1 ml trypsin-EDTA (0.05% trypsin, 0.53 mM EDTA, 14 mM NaCl in PBS) for 3 minutes at 37°C. Following incubation with trypsin cells were released from the plate by gentle agitation. One milliliter of growth medium was added, and the concentration of cells in the suspension was determined using a Coulter Counter. Cells were seeded at a density of $2.0x10^5$ cells/10 cm plate.

LdlA7, ldlA [*murine* SR-BI], CHOK1 and CHO [*murine* SR-AI] were cultured and propagated in HAMS F12 media supplemented with 5% fetal bovine serum (FBS), 50 units/ml penicillin, 50 μg/ml streptomycin and 2 mM glutamine. ldlA[*human* SR-BI], ldllA[EGFP-*human* SR-BI] and ldlA[mRFP-*human*-SR-BI], ldlA[EGFP-clathrin], ldlA[EGFP-clathrin+ mRFP-*human*-SR-BI] and ldlA[mRFP-*human*-SR-BI] cells were cultured in the same medium containing 500 μg/ml G418 (Geneticin- Gibco).

2.2.2. Long term storage of cells:

Cells released from cell culture dishes as described above were suspended in 1 ml of FBS containing 10% DMSO and allowed to freeze by storage overnight at -80°C. Frozen stocks of cells were then stored over N_2 (l) for long term storage. Frozen cell stocks were thawed quickly at 37°C and seeded onto 10 cm plates with 10 ml of the appropriate growth medium.

2.2.3. DNA constructs

DNA constructs were generated for the purpose of establishing stable cell lines expressing *human* SR-BI, EGFP and mRFP tagged *human* SR-BI.

2.2.3.1. *pEGFP-human*-SR-BI

We generated a mammalian expression vector containing enhanced green fluorescent protein (EGFP) cDNA fused to the cDNA for *human* SR-BI (*human* SR-BI, also referred to as CD36 Like Antigen 1, or CLA-1) allowing the expression of *human* SR-BI protein with EGFP fused to its amino terminus. The *human* SR-BI cDNA was amplified by polymerase chain reaction (PCR) using an expression vector containing the *human* SR-BI cDNA (provided by Dr. M. Krieger, MIT). Primers were designed to introduce a SalI and a KpnI restriction site, respectively, at each end of the cDNA. The PCR product was ligated into the pGEM-T Easy vector. After amplification in bacteria and purification, the plasmid was digested with SalI and KpnI and the *human* SR-BI fragment was ligated into the pEGFP-C1 vector (Clontech) digested with SalI and KpnI. This plasmid was amplified, purified and subjected to DNA sequencing. Nucleotides that

did not correspond to the *human* SR-BI/CLA-1 cDNA sequence (Calvo et al, 1993) were corrected by site directed mutagenesis using the Quickchange mutagenesis kit (Stratagene).

2.2.3.2. *pmRFP-human-SR-BI*

An expression vector conferring expression of *human* SR-BI tagged at its N-terminus with monomeric Red Fluorescent Protein (mRFP) was generated as follows: the mRFP cDNA was excised from pmRFP-C1 (provided by Dr. Ray Truant) using Nhe1 and BspE1. pEGFP-*human* -SR-BI was digested with Nhe1 and BspE1 to remove sequences encoding EGFP. The mRFP fragment was ligated into the vector to generate pmRFP-*human*-SR-BI.

2.2.3.3. *p-human SR-BI*

In an effort to generate DsRed tagged *human* SR-BI, the *human* SR-BI cDNA was excised from pEGFP-*human*-SR-BI by digesting with Sal1 and Kpn1 and ligated into the pDsRed-N1 vector (Clontech) also digested with Sal1 and Kpn1 (this construct was not used in the experiments presented in this thesis). A stop codon was inserted by site directed mutagenesis (Quickchange kit, Stratagene) adjacent to the last coding exon of the *human* SR-BI cDNA based on the published cDNA sequence (Calvo et al, 1993 (Genbank ID NM_005505)).

2.2.3.4. *pEGFP-Clathrin*

Plasmid encoding clathrin (light chain) fused with EGFP protein was obtained from Dr. Sergio Grinstein (University of Toronto).

2.2.3.5. *pHA-Dyn1-K44A*

Plasmid encoding dominant negative mutant of Dynamin (Dynamin K44A) with an amino terminal HA tag was also obtained from Dr. Grinstein (University of Toronto). All vector constructs were sequenced to ensure that DNA sequence was correct and in the right coding frame.

2.2.4 Transfection

Cells were cultured on 35 mm culture dishes for 1 day prior to transfection with 2-5 μg of DNA using either Lipofectin (Invitrogen, Palo Alto, CA), Lipofectamine (Invitrogen, Palo Alto, CA) or Fugene (Roche Indianapolis, IN) transfection reagent following manufacturers instructions. Medium containing transfection reagent and plasmid DNA was replaced with growth media 24 hr later. In cells transfected with pHA-Dyn1-K44A, medium was replaced with growth medium containing 3% NCLPDS, 4 hr post transfection.

2.2.5. Stable cells lines:

Cells were cultured and propagated as described in section 2.2.1.

2.2.5.1 ldlA7, CHOK1, ldlA[murine SR-BI] and CHO[mSR-AI]

All experiments were done using Chinese Hamster Ovary (CHO) cells or *ldlA7* cells. *LdlA7* cells are derived from CHO cells and lack functional low density lipoprotein (LDL) receptor. To study *murine* SR-BI (*murine* SR-BI), we used *ldlA7* cells stably transfected with *murine* SR-BI (referred to as ldlA[*murine* SR-BI] cells). *Murine*

scavenger receptor, class A type I (*murine* SR-AI) was used in a number of experiments as a control since this receptor is known to mediate internalization of acetyl-LDL via endocytosis involving clathrin coated pits. For these experiments, CHO cells stably transfected with *murine* SR-AI (referred to as CHO[*murine* SR-AI] cells) were used. CHOK1, CHO[*murine* SR-AI], ldlA7 and ldlA[*murine* SR-BI] cells were provided by Dr. Monty Krieger (Massachusetts Institute of Technology).

CHO[*murine* SR-AI] and ldlA[*murine* SR-BI] cells were subjected to fluorescence activated cell sorting (FACS) after incubation with DiI-Ac-LDL or DiI-HDL, respectively, in order to generate populations of cells with high levels of expression of SR-AI or SR-BI. Cells ($1.6x10^6$) were seeded on a 10cm dish in growth media containing 3% Lipoprotein deficient serum (NCLPDS) for two days. On day three, prior to FACS, ldlA[*murine* SR-BI] cells were incubated with 5 μg/ml of DiI-HDL, and CHO[*murine* SR-AI] cells with 5 μg/ml of DiI-Ac-LDL for 2 hr at 37°C (details of fluorescent lipid uptake assay described in section 2.2.8). Samples of Cells were prepared for fluorescence activated cell sorting (details in section 2.2.13.1). Samples were filtered through 0.5 micron nylon mesh before cell sorting. Cells with high accumulation of fluorescent lipid (DiI) were sorted away from the rest using FACS Vantage (BD) cell sorter. Sorted cells were collected in growth media. These cells were propagated in tissue culture in growth medium (Hams F12 + 5% FBS) (three passages) and frozen down in small aliquots to be used later. Data from fluorescence activated cell sorting of ldlA[*murine* SR-BI] is plotted in Figure 6 (A). Black histogram represents cell population

prior to sorting and red histogram represents a small number of sorted cells analyzed right after sorting.

2.2.5.2. *ldlA[human SR-BI], ldlA[EGFP-human SR-BI], ldlA[mRFP-human-SR-BI]*

We established stable cell lines expressing *human* SR-BI (ldlA[*human* SR-BI]), enhanced green fluorescent protein tagged *human* SR-BI (ldlA[EGFP-*human* SR-BI]) and monomeric Red Fluorescent Protein tagged *human* SR-BI (ldlA[mRFP-*human*-SR-BI]). CHO derived ldlA7 cells were transfected with p*human*-SR-BI, pEGFP-*human*-SR-BI and pmRFP-*human*-SR-BI (described in section 2.2.3.1 to 2.2.3.3) using Lipofectin transfection reagent, according to manufactures instructions to make stable cell lines. Cells were grown on 6 cm tissue culture dishes in growth media at a density of $3.5x10^3/cm^2$. Four micrograms of DNA and 6 µl of Lipofectin reagent was used for transfection. Transfected cells were subjected to selection pressure, by culturing in selection media containing 100 µg/ml of Geneticin. To enrich these cell lines with cells expressing *human* SR-BI (mRFP tagged or untagged), cells were sorted using fluorescence activated cell sorting, based on their ability to take up DiI from DiI-HDL (as described earlier in section 2.2.5.1). Cells expressing EGFP-tagged *human* SR-BI were sorted based on their EGFP-fluorescence. Data from fluorescence activated cell sorting of ldlA[*human* SR-BI], ldlA[mRFP-*human*-SR-BI] and ldlA[EFGP-*human* SR-BI] is plotted in Figure 6 (B-D). Black histogram represents cell population prior to sorting and red histogram represents a small portion of sorted cells analyzed right after sorting.

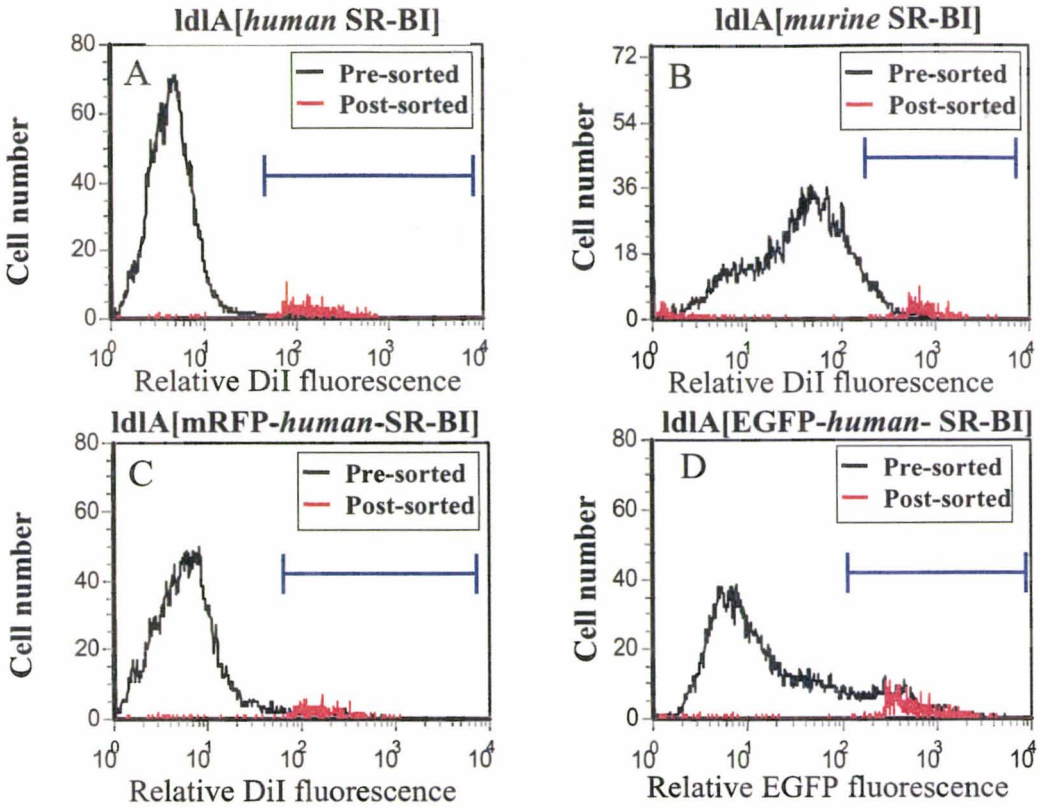

Figure 6: Fluorescence activated sorting of ldlA[*human* SR-BI], ldlA[*murine* SR-BI], ldlA[mRFP-*human*-SR-BI] and ldlA[EFGP-*human*-SR-BI] cells:
ldlA[*human* SR-BI] (A), ldlA[*murine* SR-BI] (B), and ldlA[mRFP-*human* SR-BI] (C) cells were incubated with 5µg/ml of DiI labeled HDL for 2 hours at 37°C to allow SR-BI mediated DiI up take in cells. Cells were then washed with PBS containing 0.5% BSA, trypsinized and prepared for fluorescence activated cell sorting using a FACS Vantage. LdlA[EGFP-*human*-SR-BI] cells were prepared for fluorescence activated cell sorting without prior incubation with DiI-HDL. A portion of each cell suspension was analyzed prior to cell sorting, to get an estimate of distribution of SR-BI and SR-AI expression within populations (black; "Pre-sorted"). Black histogram represents the distribution of DiI uptake in the population of cell prior to cell sorting. FACS vantage was set up to sort cells with highest accumulation of DiI (marked by the horizontal blue line) away from the rest of the population. Sorted cells were collected into 3 ml tubes containing growth media. After the sorting was complete, a small sample from the of each sorted population of cells was analyzed on the FACS Vantage and plotted as the red histograms (red; "Post-sorted"). Red histograms give an initial assessment of the success of fluorescence activated cell sorting in enriching the population with high expressing cells. ldlA[EGFP-*human*-SR-BI] cells were sorted based on the level of EGFP fluorescence.

2.2.5.3. *ldlA[EGFP-clathrin], ldlA[EGFP-clathrin+ mRFP-human-SR-BI] and ldlA[mRFP-human-SR-BI]*

LdlA7 cells were transfected with plasmids encoding EGFP tagged clathrin (pEGFP-clathrin) or mRFP tagged *human* SR-BI, or both pEGFP-clathrin and mRFP-*human*-SR-BI using Lipofectamine 2000 (Invitrogen). Post transfection, cells were kept under selection pressure by growing in media containing (500 μg/ml) Geneticin (G418).

2.2.6. Preparation of maleyl-BSA

BSA (Sigma. St. Louis, MO) was dissolved in 7 ml of LDL buffer (0.15 M NaCl and 0.3 mM EDTA, pH 7.4). Saturated sodium borate (13 ml) was slowly added to the solution while stirring. Maleic anhydride (200 mg) was added to the solution in small amounts, maintaining the pH between 8.5-9. The reaction mixture was then allowed to stir for 1 hr prior to dialysis (30 kDa MW cut off dialysis tubing) against 6 liters of LDL buffer at 4°C with six changes. After dialysis, the solution was filter sterilized (0.2 μm) and the protein concentration was determined using the BCA assay (Pierce, Rockford, IL).

2.2.7. Preparation of DiI labeled AcLDL and HDL

2.2.7.1. DiIAcLDL

A mixture of LDL (5.25 mg protein) and 10.5 ml of *human* lipoprotein deficient serum (generous gift from Dr. Monty Krieger, MIT) was filter sterilized (0.45μm). Fluorescent lipid 1,1'-dioctadecyl-3,3,3',3'- tetramethylindocarbocyanine perchlorate

('DiI'; $DiIC_{18}$) (0.79 mg of a 3 mg/ml solution in DMSO) was added and the mixture was incubated for 17 hr at 37°C in the dark. After 17 hr, the mixture was placed on ice and 0.853 g of KBr was dissolved in it to bring the density to 1.063 g/ml). The mixture was subjected to centrifugation at $4.68x10^4$ rpm in a Beckman ultracentrifuge using a Ti80 rotor for 23 hr. DiI-LDL was collected from the top of the tube and was dialyzed (30 kDa MW dialysis tubing) against 6 liters of LDL buffer at 4°C (three changes). After dialysis, DiI-LDL was acetylated at 4°C by the addition of an equal volume of saturated sodium acetate (total volume of reaction 6.6 ml) and 5x 46.2 µl aliquots of acetic anhydride (at 10 min intervals) at 4°C while stirring. After the last addition of acetic anhydride, the reaction was allowed to continue with stirring for 1 hr at 4°C. The mixture was then dialyzed against LDL buffer as above.

2.2.7.2. DiI HDL

A mixture of HDL (5.25 mg protein) and 10.5ml of *human* lipoprotein deficient serum (generous gift from Monty Krieger, MIT) was filter sterilized (0.45µm). Fluorescent lipid 1,1'-dioctadecyl-3,3,3',3'- tetramethylindocarbocyanine perchlorate ('DiI'; $DiIC_{18}$) (0.79 mg of a 3 mg/ml solution in DMSO) was added to the mixture. 15 ml falcon tube containing the mixture was flushed with $N_{2\,(g)}$ and incubated for 17 hr at 37°C in the dark. After 17 hr, the mixture was placed on ice. Ten milliliter mixture were transferred to a 10 milliliter falcon tube containing 3.37grams of KBr (calculated density of the solution would be 1.063 g/ml). Tube containing the mixture was flushed with N_2 (l). The mixture was subjected to centrifugation ($4.68x10^4$ rpm) in a Beckman

ultracentrifuge using a Ti80 rotor for 23 hr. DiI-HDL was collected from the top of the tube and was dialyzed (30 kDa MW dialysis tubing) against 6 liters of LDL buffer (that had been flushed with N_2 (l)) at 4°C (six changes). After dialysis, HDL was stored in cryovials over N_2 (l) at 4°C in the dark.

2.2.8. Fluorescent lipid uptake assay

Cells ($5.0x10^4$in 35mm dishes were cultured in medium B (HAM's F12 media containing 3% NCLPDS, 50 units/ml penicillin, 50 µg/ml streptomycin and 2 mM glutamine) for two days. On day three, cells were washed once with HAM's F12 without additives and incubated with 5 µg/ml DiI-HDL or DiI-Ac-LDL in medium C (HAM's F12 containing 50 units/ml penicillin, 50 µg/ml streptomycin, 2 mM glutamine and 0.5% BSA) for 2 hr at 37°C. Cells were then washed with twice with cold PBS containing 0.5% BSA and once with warm PBS prior to gentle trypsinization (3 min at 37°C). Cell samples were prepared for flow cytometry as described in section 2.2.13.1. Cells were analyzed by flow cytometery as described in section 2.2.13.2.

2.2.9. Lipid uptake assay in cells depleted of intracellular potassium

In some experiments, intracellular potassium was depleted prior to measurement of fluorescent lipid uptake. As above, cells were cultured for two days prior to the experiment. On day 3, cells were washed with HAM's F12 without additives, and then subjected to hypotonic shock by incubation in 1 ml of a 1:1 mixture of HAM's F12 and water at 37°C for 5 min. Cells were then incubated for 1 hr at 37°C in K-free medium

(140 mM NaCl, 1mM $CaCl_2$, 1 mM $MgCl_2$, 5.5 mM glucose, 0.1%BSA and 20 mM HEPES, pH 7.4). Control cells were incubated in K-containing medium (K-free medium, supplemented with 10 mM KCl). Uptake of DiI from DiI-Ac-LDL or DiI-HDL was then performed as described above, except that K-free or K-containing media (supplemented with 5 μg/ml of DiI-labeled lipoprotein) was used for incubation. Cell samples were prepared for flow cytometry as described in section 2.2.13.1. Cells were analyzed by flow cytometery as described in section 2.2.13.2.

2.2.10. Lipid uptake assay in cells treated with hypertonic shock

Cells were cultured in medium B (as described in section 2.2.8). On day three, growth media was removed and cells were washed with Ham's F12 without additives. Cells were incubated for with one ml of hypertonic (HAM's F12 containing 0.5 % BSA and 0.4 M sucrose) or control media (HAM's F12 containing 0.5 % BSA) for 1 hr at 37°C. Uptake of DiI from DiI-Ac-LDL or DiI-HDL was then performed (as described in 2.2.8), except that hypertonic or control media were used as incubation media. Cell samples were prepared for flow cytometery (as described in section 2.2.13.1). Cells were analyzed by flowcytometery (as described in section 2.2.13.2).

2.2.11. Treatment of cells with cytochalasin D or colchicine

Cells were cultured in medium B as described above in section 2.2.8. On day 3, medium B was replaced with 2 ml of either fresh medium B (control) or with medium B supplemented with either 10 μM cytochalasin D or 10 μM colchicine and cells were

incubated for 2 hr at 37°C. Uptake of DiI from DiI-Ac-LDL or DiI-HDL was then performed as described above in section 2.2.8, except that medium B either lacking or containing 10 mM cytochalasin D or colchicine was used (concentrations of DiI-HDL and DiI-Ac-LDL were 5 μg/ml). Cell samples were prepared for flow cytometery (as described in section 2.2.13.1). Cells were analyzed by flow cytometry (as described in section 2.2.13.2). Alternatively, cells were imaged by live cell fluorescence microscopy as described below.

2.2.12. Fluorescence microscopy

2.2.12.1. Preparation of glass bottom plates

Cell culture dishes (35 mm) with glass bottom were prepared by cutting holes into the bottom of the dishes and gluing glass cover slips to the bottom of the dishes. Cover slips were pre-washed with water and 70% ethanol. Once the glue was dry dishes were rinsed with water and soaked in 95% ethanol in sterile tissue culture hood with UV light on for 2-4 hr. Cover slip surface was coated with poly-*D*-lysine, by incubation with 200 μl of poly-*D*-lysine solution for 5 min. Poly-*D*-lysine solution was removed and dishes were allowed to dry for 24 hr before use (adapted from Howell and Truant, 2002).

2.2.12.2. Inverted fluorescence microscope

Zeiss Inverted microscope Axiovert 200M was used for fluorescent imaging of cells. Zeiss filter set 13 was used to detect FITC, Alexa 488 and EGFP fluorescence, filter set 01 was used for DAPI and filter set 10 was used for DiI and mRFP fluorescence.

Images were taken using a (Zeiss Axiocam HRc) camera attached to the microscope, saved as Axiovision files which were later exported as Tagged Image Files and included in the thesis.

2.2.12.3. Laser confocal microscope

Zeiss LSM510 was used for laser confocal microscopy. Prior to imaging cells were fixed as described in section 2.2.14.1.

2.2.12.4. Live cell imaging

Nikon-Hamamatsu inverted live-cell fluorescence microscope was used to obtain live cell images of tagged SR-BI and DiI labeled ligands in cells. For live cell imaging cells were imaged on glass bottom ΔT dishes (Bioptics, Beaver Falls, PA) which were heated to 37° C using a heated stage apparatus, while imaging. Cells were kept in media containing 25 mM HEPES buffer during imaging.

2.2.13. Analysis of cell associated fluorescence using a flow cytometer

2.2.13.1. Sample preparation

Cells were released from the plates by trypsinization (as described in section 2.2.1). Trypsin was quenched by using trypsin inhibitor. Cells were then diluted in 2 ml of ice cold FACS buffer (0.5% BSA and 0.1% sodium azide in PBS) in 5 ml falcon tubes (BD 2058) and centrifuged for 15 minutes at 500xg at room temperature. Pelleted cells were washed with ice cold FACS buffer, then resuspended in 250 µl of ice cold FACS buffer. Cells were kept on ice until analyzed by the flow cytometer.

2.2.13.2. Sample analysis

DiI fluorescence was read in the FL2 channel (detects emission wavelengths between 565-585 nm) and EGFP fluorescence was read in FL1 channel (detects emission wavelengths between 505-525 nm) using a FACScan. When detecting EGFP and DiI fluorescence in the same cell sample compensation was used to eliminate DiI signal from the FL1 and EGFP signal from FL2. ldlA[*murine* SR-BI] cells incubated with DiI-HDL, and ldlA7 expressing EGFP-*human* SR-BI were used for compensation.

2.2.13.3. Preparation of cell lysates, protein determination, SDS-PAGE and immunoblotting:

Cells were washed with ice cold PBS twice and collected into 1.5 ml microcentrifuge tubes by scraping in 200 µl of ice cold Lysis Buffer (0.2 X PBS containing, 0.1% Triton, 1 mM PMSF, 20 µg/ml aprotinin, 10 µg/ml leupeptin and 10 µg/ml pepstatin). Lysates were subjected to centrifugation 14,000 rpm in a microfuge for 10 min at 4°C. Supernatants were collected and stored at -80°C until used. Protein concentrations were determined using the BCA Protein Assay (Pierce) using BSA as a standard. Protein (15 µg) in cell lysates was denatured by boiling for 5 min in Laemmli sample buffer (0.125 M Tris-HCl pH 6.8, containing 5% sodium dodecylsulfate (SDS), 8.9% (v/v) 2-mercaptoethanol, 9% (v/v) glycerol and 0.05% bromophenol blue. Proteins were subjected to SDS-polyacrylamide gel electrophoresis using either an 8% or a 12.5% acrylamide separating gel (375 mM Tris-HCL pH 8.8, 0.1% SDS) and a 4% acrylamide

stacking gel (125 mM Tris-HCl pH 6.8, 0.1% SDS) (acrylamide:bis-acrylamide ratio of 30:0.8) (Laemmli, 1970). Electrophoresis was performed for 45min at 200 V using 25 mM Tris, 192 mM glycine (pH 8.3) containing 1% SDS. After SDS-PAGE, proteins on the polyacrylamide gels were electrophoretically transferred onto PVDF membrane using 25 mM Tris, 192 mM glycine, pH 8.3 as the transfer buffer, at 4°C for 30 min at 24 V using an Idea Scientific transfer apparatus. Prior to transfer, PVDF membrane was soaked in methanol for 20 sec, water for 2 min and transfer buffer for 10 minutes. Polyacryamide gels were soaked in transfer buffer for 5 min.

PVDF membranes were blocked by incubation at 37°C for 1 hr in PBS-T (PBS containing 0.1% Tween-20) containing 5% skim milk powder. Membranes were washed 2 x with water and 3 x PBS-T (10 min/wash) with constant agitation at room temperature. Incubation with primary antibodies (dilutions indicated in Figure legends) in 5 ml of PBS-T for 1 hr at room temperature with constant rocking. Membranes were washed as described above in PBS-T. Incubation with HRP conjugated goat anti-rabbit secondary antibody (PerkinElmer Life Sciences, Boston, MA) diluted 1: 5000 in PBS-T, for 1 hr at room temperature. Membranes were washed in PBS-T as described above and bound antibodies were detected using the Western Lightning Enhanced Chemiluminescence Reagent Plus kit (PerkinElmer Life Sciences, Boston, MA). The luminescence on the blot was either imaged using a Kodak Image Station 440CF for quantitative analysis or by exposure to autoradiography film (Kodak X-omat XAR5) for qualitative analysis of proteins.

2.2.14. Immunofluorescence assay

2.2.14.1. Fixing and permeabilization of cells

Before cells were plated on dishes, dishes were washed with autoclaved water and then with PBS. Cells were washed three times with PBS, incubated with 2.5% paraformaldehyde for 30 min at room temperature, then washed with PBS three times. After cells were fixed, they were incubated for 5 min with 100 mM NH_4Cl and washed with PBS. Cells were permeabilized 0.1% TritonX-100 on ice for 5 min.

2.2.14.2. Immunofluorescence

Cells were blocked with 10% Fetal Bovine Serum (FBS) for 30 min at room temperature. Cells were treated with rabbit anti-mouse anti HA tag antibody (Santa Cruz Biotechnology, CA) (1:500 dilution, in PBS containing 0.1% Tween 20) for 1 hr at room temperature, then with Alexa 488 conjugated goat anti rabbit secondary (1:1000 dilution in PBS containing 0.1% Tween 20) for 1 hr at room temperature. Cells were washed with PBS. Cells were kept in the dark prior to imaging.

3. Results

3.1. Generation of stable cell lines expressing human SR-BI

Previous studies have reported that SR-BI can be detected in endocytic compartments. In one study SR-BI was shown to co-localize with transferrin in intracellular compartments during transferrin uptake (Silver et al., 2001[b]). In order to study the dynamics of SR-BI's sub-cellular distribution using fluorescence microscopy, I generated cell lines expressing SR-BI tagged with either enhanced green fluorescent protein or monomeric red fluorescent protein on the amino terminus. To follow the dynamics of SR-BI mediated lipid uptake in live cells, I used lipoprotein ligands of SR-BI (HDL and acetylated-LDL) containing a fluorescent lipid, called DiI-C18 ("DiI").

3.1.1. Expression of human SR-BI in ldlA7 cells

Expression constructs for *human* SR-BI tagged with enhanced green fluorescent protein (EGFP) (pEGFP-*human*SR-BI), monomeric red fluorescent protein (mRFP) (pmRFP-*human*SR-BI) or untagged *human* SR-BI (p*human*SR-BI) were generated as described above (*Materials and Method 2.2.3. DNA constructs*). To analyze the function and dynamic localization of untagged and tagged *human* SR-BI in cells, these plasmids were transfected into ldlA7 cells. These are Chinese hamster ovary (CHO) derived cells that lack a functional LDL receptor (provided by Dr. Monty Kreiger, (Acton et al., 1994)). To detect tagged and untagged *human* SR-BI in transfected ldlA7 cells, immunoblotting was performed 48 hr post-transfection on extracts of transfected cells, using an antibody against a peptide derived from the cytoplasmic carboxyl terminus of

murine SR-BI *(Materials and Method, 2.2.13.3. Preparation of cell lysates, protein determination, SDS-PAGE and Immunoblotting).* "Mock" transfected ldlA7 cells (no plasmid) and ldlA[*murine* SR-BI] cells (transfected ldlA7 cells stably over-expressing *murine* SR-BI (Acton et al, 1996) were used as negative and positive controls, respectively. Figure 7 shows that no band was detected in the mock-transfected ldlA7 cell extract (lane 2). However, as expected, a single major band was detected in the each of the extracts from ldlA[*murine* SR-BI] cells (lane 1) and from ldlA7 cells transfected with p*human* SR-BI (lane 3); this band migrated slower than the 79 kDa molecular weight marker, consistent with SR-BI's reported molecular weight of 85 kDa (Acton et al., 1996; Babitt et al., 1997). In contrast, a band of lower mobility was detected in the extract from ldlA7 cells transfected with pEGFP-*human*-SR-BI (lane 4). This band migrated with mobility close to that of the 116 kDa molecular weight standard, consistent with the expected size (~27 kDa) of the EGFP polypeptide fused to the amino terminus of SR-BI.

To visualize the distribution of tagged SR-BI by fluorescence microscopy, cells were cultured on glass bottomed culture dishes (method of (Howell and Truant, 2002)) coated with poly-D-Lysine. Krieger and colleagues (Babitt et al., 1997) first demonstrated, by immunofluorescence in permeabilized ldlA[*murine* SR-BI] cells, that SR-BI was distributed in a punctate pattern over the body of cells and accumulated on the edges of cells at regions of cell-cell contact (see Fig 8 panel M; immunofluorescence performed by Judy Lin). To determine if EGFP and mRFP-tagged versions of *human* SR-BI had a similar pattern of distribution in cells, ldlA7 cells grown on glass bottomed dishes were transfected with either pEGFP-*human*-SR-BI, pmRFP- *human*-SR-BI or both

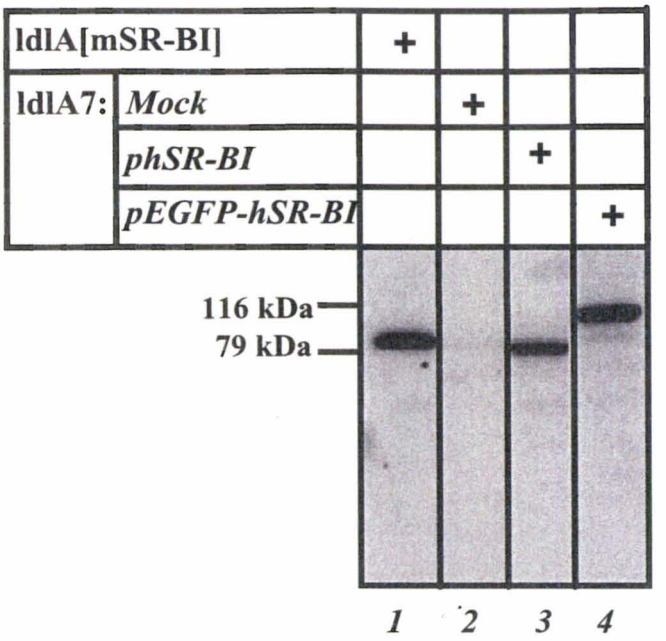

Figure 7. Immunoblot analysis of EGFP-tagged or untagged *human* SR-BI expression in transfected ldlA7 cells. LdlA7 cells were transfected without DNA (mock) lane 2, with untagged *human* SR-BI (lane 3) or EGFP tagged human SR-BI (lane 4) expression vectors. Cells were harvested 48 hrs post transfection. ldlA[*murine* SR-BI] cells stably expressing *murine* SR-BI were used as a positive control for SR-BI expression. Cell lysates were prepared in 0.2x strength PBS, containing 0.1% tritionX-100, PMSF and protease inhibitors (*as described in Methods section 2.2.12.3.*) Samples were subjected to SDS PAGE, using a 10% polyacrylamide separating gel, proteins were electrophoretically transferred to PVDF. Immunoblotting with a rabbit an anti-SR-BI antibody (495 anti-SR-BI provided by Dr. Monty Kreiger, (Massachusetts Institute of Technology)) (1:50,000 dilution) and an HRP conjugated anti-rabbit secondary antibody (1:5000) was performed. Proteins were visualized using ECL reagent and imaging the blot on using a Kodak Image Station 440CF. The positions of protein standards of 116 and 79 k Da are shown on the left.

of these plasmids. Representative fluorescence and corresponding differential interference contrast (DIC) images are shown in Figure 8. Both EGFP-*human*-SR-BI (panels E, H and K) and mRFP-*human*-SR-BI (panels A, G and J) displayed similar distributions to the immunofluorescence distribution of *murine* SR-BI (panel L). No green fluorescence was visible in cells transfected with pmRFP-*human*-SR-BI (panel B) and no red fluorescence was visible in cells transfected with pEGFP-*human*-SR-BI (panel D). When cells were transfected with both pEGFP-*human*-SR-BI and pmRFP-*human*-SR-BI, the EGFP and mRFP fluorescence distribution was indistinguishable (G and H, J and K). Therefore, tagging *human* SR-BI with either EGFP or mRFP did not appear to affect its distribution in cells.

ldlA[mRFP- *human* SR-BI] and ldlA[EGFP- *human* SR-BI] cells seeded on glass bottom plates, were used for live cell imaging at 37°C (*Materials and Method 2.2.12.4. Live cell imaging).* It appears that tagged SR-BI is in dynamic structures in the cells that move in the three dimensional space of the cell. These vesicles have characteristics similar to those of endocytic vesicles moving to and from cell periphery. Video images of the vesicular movement can be seen in the supplementary material provided on the CD. These observations suggested that endocytosis may play a role in the function of SR-BI in cells.

3.1.2. Fluorescent protein tagged SR-BI is able to take up lipid from HDL

To test if tagged *human* SR-BI was able to take up lipid from HDL, cells transfected with pEGFP-*human*-SR-BI were incubated with HDL loaded with

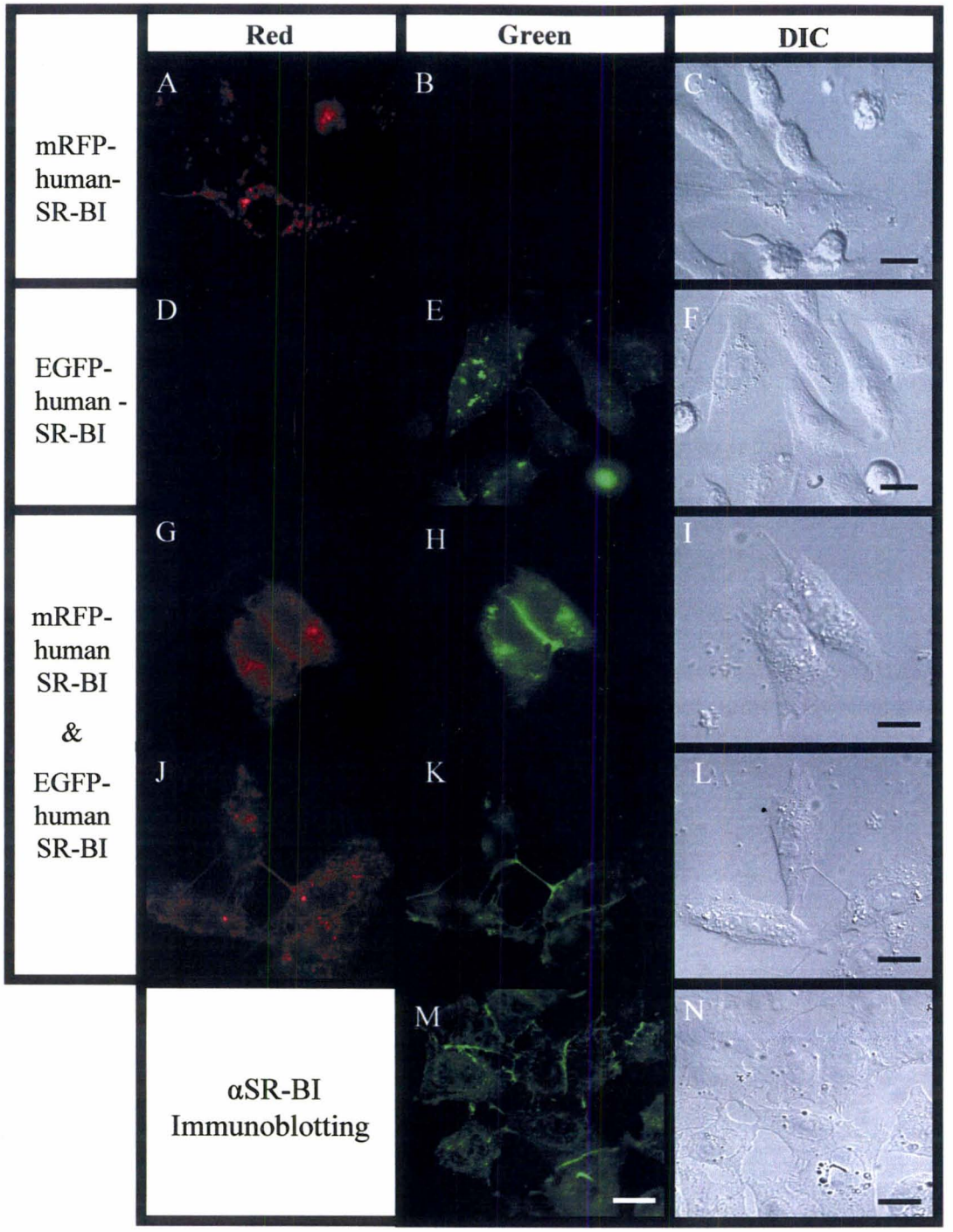
Red
Green
DIC
A
B
C
mRFP-human-SR-BI
D
E
F
EGFP-human - SR-BI
G
H
I
mRFP-human SR-BI
&
EGFP-human SR-BI
J
K
L
αSR-BI Immunoblotting
M
N

Figure 8: Fluorescence localization of EGFP or mRFP-tagged *human* SR-BI in transfected CHO cells: LdlA7 cells seeded on glass bottom dishes, were transfected with a plasmid encoding mRFP (pmRFP-*human* SR-BI) (top row A-C), EGFP tagged human SR-BI (pEGFP-*human* SR-BI) (second row D-F) or co-transfected with both pmRFP-*human* SR-BI and pEGFP-*human* SR-BI (third and fourth rows G-L). mRFP fluorescence was detected using Zeiss filter set 10 (column on the left, panels A, D, G and J), and EGFP or alexa 488 fluorescence was detected using Zeiss filter set 13 (middle column, panels B, E, H, K and M) at 63x magnification, using an inverted fluorescence microscope. DIC images were taken under bright field and are shown in panels C, F, I, J and N. No mRFP fluorescence was detected using the EGFP filter (B), and no EGFP fluorescence was detected using the mRFP filter (D). The distribution of untagged *murine* SR-BI in fixed ldlA[*murine* SR-BI] detected by indirect immunofluorescence (M and N) was performed by Judy Lin and is shown in row five (Scale bar = 20μm)

the fluorescent lipid DiI for 2 hr at 37°C (*Materials and Method 2.2.8. Fluorescent lipid uptake assay;* adapted from (Acton 1996)). Accumulation of DiI within cells was measured by flow cytometry (*Materials and Method 2.2.13. Analysis of cell associated fluorescence using a flow cytometer*). As a positive control for SR-BI mediated lipid uptake, ldlA[*murine* SR-BI] cells were incubated with DiI-HDLcontrol. Figure 9 shows the results of two-color flow cytometric analysis of DiI fluorescence (vertical axis. FL2 channel; emission 565-585 nm) and EGFP fluorescence (horizontal axis. FL1 channel; emission 505-525 nm). Approximately $1x10^5$ cells (each cell represented by a dot on the plot) were analyzed from each sample. As expected, ldlA[*murine* SR-BI] cells incubated with DiI-HDL (panel A), displayed high DiI fluorescence accumulation without apparent EGFP fluorescence. LdlA[EGFP-*human* SR-BI] cells incubated without DiI-HDL displayed high EGFP fluorescence but no apparent DiI fluorescence (panel B). When ldlA[EGFP-*human* SR-BI] cells were incubated with DiI-HDL (panel C), they displayed high DiI and EGFP fluorescence. There was a positive correlation between DiI and EGFP fluorescence demonstrating that the level of HDL lipid uptake was dependent on the level of expression of EGFP-*human* SR-BI. This demonstrates that EGFP-tagged *human* SR-BI was able to mediate cellular uptake of HDL lipids.

Figure 9 shows that when using DiI fluorescence as a marker of lipid uptake in cells, flow cytometry can be a powerful analytical technique to quantify SR-BI mediated lipid uptake in individual cells in large populations. We made use of this methodology to select for stably transfected ldlA[*murine* SR-BI], ldlA[*human* SR-BI], ldlA[EGFP-*human* SR-BI], ldlA[mRFP-*human*-SR-BI] cells and CHO[*murine SR-AI*] cells with high

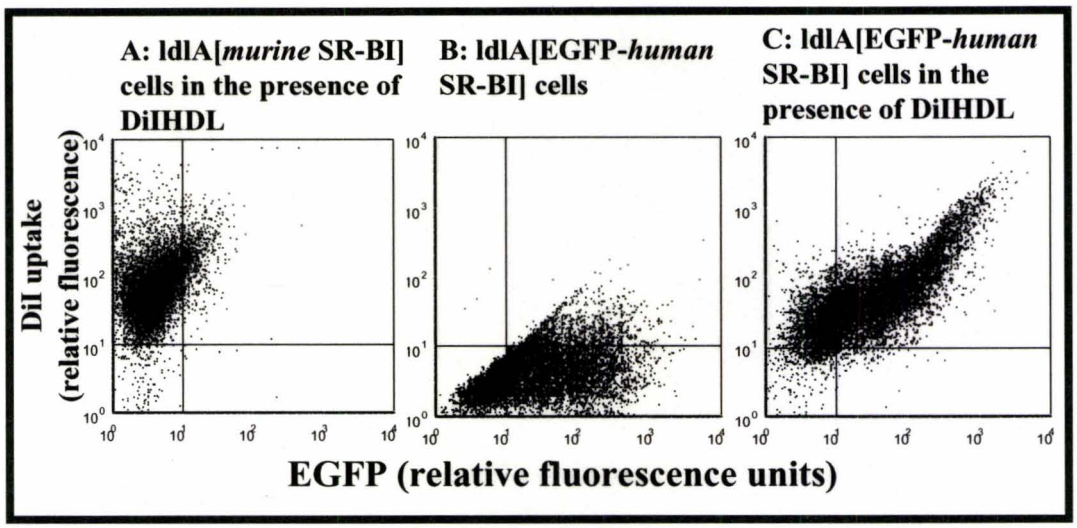

Figure 9: Uptake of DiI from DiI-HDL by cells expressing tagged *human* SR-BI: LdlA7 cells expressing either *murine* SR-BI (A) or EGFP-tagged *human* SR-BI (C) were incubated with DiI-HDL (5 μg/ml) for 2 hours at 37 °C. Another sample of cells expressing EGFP-tagged *human* SR-BI was incubated in the absence of DiI-HDL (B). Cells were washed with ice cold PBS containing 0.5% BSA to remove unbound DiI-HDL. Cell were then removed from plates by gentle trypsinization, washed with ice cold PBS containing 0.5% BSA and 0.1% sodium azide, and resuspended in 250 μl of the same. DiI (vertical axis; emission at 575 nm) and EGFP fluorescence (horizontal axis; emission at 508 nm) was determined by flow cytometry using a FACScan instrument .

levels of transgene expression. Briefly, ldlA[*murine* SR-BI], ldlA[*human* SR-BI], and ldlA[mRFP-*human*R-BI] cells were incubated with DiI-HDL, and CHO[*murine SR-AI*] cells with DiI-acetylated-LDL (DiI-Ac-LDL) for 2 hr at 37°C. LdlA[EGFP- *human*-SR-BI] cells were not incubated with DiI-containing lipoproteins. Cells were subjected to fluorescence activated cell sorting (FACS), based on either the accumulation of DiI fluorescene in cells or the level of EGFP fluorescence (see *Materials and Method section 2.2.5.2 and Figure 6*). For each cell type, the sorted populations with the highest levels of DiI or EGFP fluorescence were collected and expanded in culture.

DiI uptake from either DiI-HDL or DiI-Ac-LDL was then analyzed in the resulting populations of cells. Either untransfected or the sorted and expanded populations of ldlA[*human* SR-BI], ldlA[*murine* SR-BI], ldlA [EGFP-*human*-SR-BI] and CHO[*murine* SR-AI] cells were incubated with DiI-HDL or DiI-Ac-LDL for 2 hr at 37°C and analyzed for accumulation of DiI fluorescence by flow cytometry. Figure 10 shows the histograms of cell number (vertical axis) versus DiI fluorescence (horizontal axis). DiI fluorescence in the transfected and sorted cells (red histograms in each panel) was clearly greater than the level of fluorescence in corresponding untransfected control cells (black histograms). CHO[*murine SR-AI*], ldlA[*murine* SR-BI] and ldlA[EGFP-*human*-SR-BI] samples each displayed a major population of cells with a mean DiI fluorescence 10-fold higher than that of the corresponding untransfected cells (black curves). In addition to the major population, ldlA[*murine* SR-BI] and CHO[*murine* SR-AI] samples also contained minor populations (shoulders on left hand sides of red curves) that appeared to correspond to untransfected cells. The ldlA[*human* SR-BI] sample (panel A,

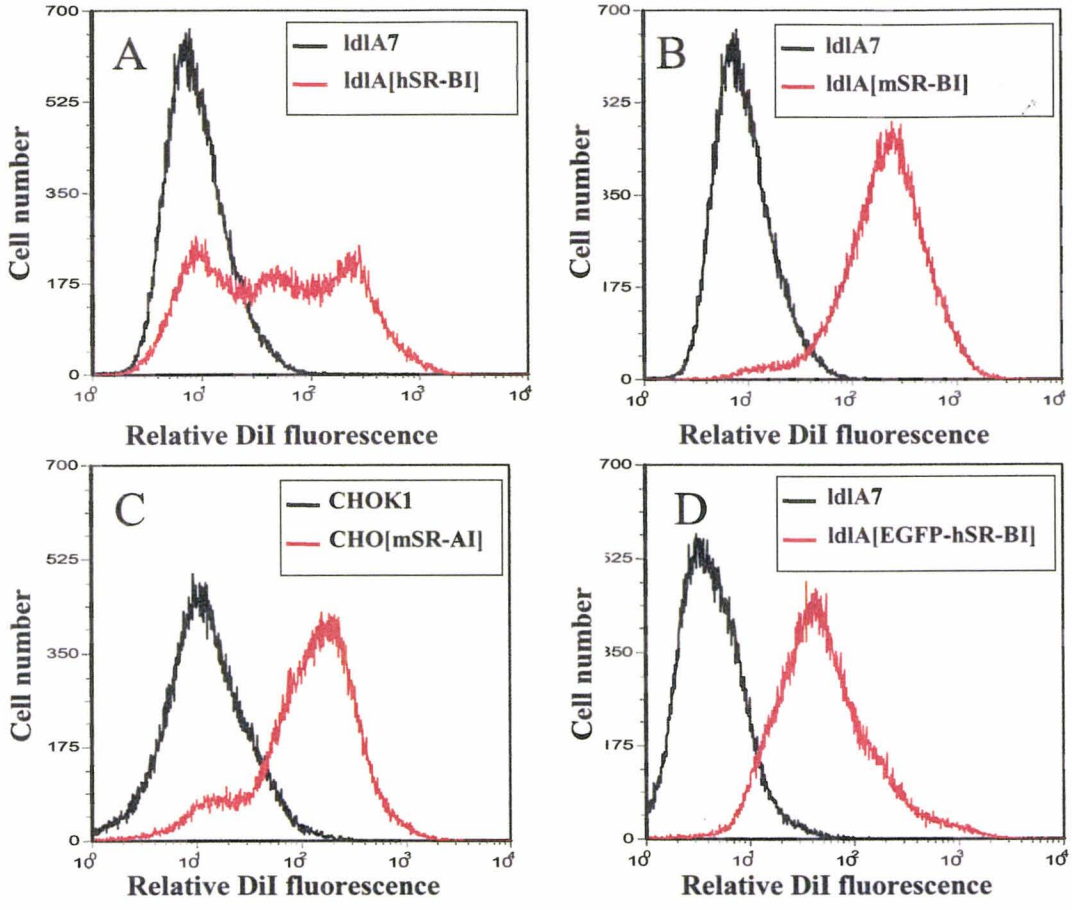

Figure 10: Fluorescence activated cell sorting of ldlA[*human* SR-BI], ldlA[*murine* SR-BI], CHO[*murine* SR-AI] and ldlA[EFGP- *human*-SR-BI] for DiI uptake activity or EGFP expression. Fluorescence activated cell sorting was used to enrich populations of transfected ldlA[*human* SR-BI], ldlA[*murine* SR-BI], CHO[*murine* SR-AI] and ldlA[EFGP- *human*-SR-BI] cells for those expressing high levels of activity (sorting for DiI uptake) or fluorescent protein expression (sorting for EGFP). Sorting was described in section 2.2.5.2 (also see figure 6). Sorted cells were propagated in tissue culture. To test the level of enrichment in cells, sorted ldlA[*human* SR-BI] (A), ldlA[*murine* SR-BI] (B) and CHO[*murine* SR-AI] (D) cells were incubated with 5µg/ml of DiI- HDL while sorted CHO[*murine* SR-AI] cells (C) were incubated with DiI-Ac-LDL for 2 hours at 37°C (see section *2.2.7*). Untransfected ldlA7 (panels A, B and D) or CHO cells (panel C) (incubated with appropriate DiI-lipoproteins) were included as negative controls. DiI uptake was detected by flow cytometry (*as described in method section 2.2.1.2*). Data is plotted as cell number vs. DiI fluorescence. Red histograms show DiI fluorescence in transfected and sorted cells. Black histograms show the DiI fluorescence in in untransfected control cells.

red histogram) appeared to contain three populations of cells (three different median or peak fluorescence values). One of these populations appears to correspond to untransfected ldlA7 cells. This suggests that this population of cells is comprised of three distinct subpopulations with different expression levels. Time constraints did not allow for further enrichment of these cells. The mean fluorescence of the entire population however, is at least 10-fold higher than that of corresponding untransfected cells.

3.2. Effects of blocking endocytosis in cells

As mentioned previously, the depletion of cellular potassium and exposure to hyperosmotic conditions have been used extensively as means of disrupting endocytic pathways in cells. To assess the role of endocytosis in SR-BI-mediated lipid uptake from lipoproteins, we measured the effects of depleting cellular potassium or exposing cells to hyperosmotic conditions on lipid uptake from two SR-BI ligands: HDL and Ac-LDL. We monitored the effects of these treatments on DiI-Ac-LDL uptake by CHO[*murine* SR-AI] cells because *murine* SR-AI (scavenger receptor class **A** type 1) is known to mediate Ac-LDL internalization via clathrin dependant endocytosis (Brown et al., 1979). We also monitored the uptake of fluorescent cholera toxin subunit B (CT-B) in untransfected CHO cells. CT-B uptake is dependent on the ganglioside GM1, a component of caveolae on the cell surface (Gilbert et al., 1999). Therefore CT-B uptake is often used as a measure of caveolar (or lipid raft) mediated endocytic pathways.

3.2.1. Effect of intracellular potassium depletion on SR-BI mediated lipid uptake from HDL and AcLDL

Cells (CHOK1, CHO[*murine* SR-AI], ldlA7, ldlA[*murine* SR-BI] and ldlA[*human* SR-BI]) were cultured in medium containing 3% newborn calf lipoprotein deficient serum (NCLPDS) for two days. On day three, cells were depleted of potassium by being subjected to hypotonic shock (5 minutes at 37°C), followed by incubation in media lacking potassium (1 hr at 37°C). Control cells were incubated with solution containing 10mM KCl following a hypotonic shock. Cells were then incubated with 5 μg/ml of DiI-HDL or DiI-Ac-LDL in the absence or presence of potassium (*Materials and Method 2.2.9. Lipid uptake assay in cells depleted of intracellular potassium).* In some samples, a 40-fold mass excess (200 μg/ml) of maleyl-BSA was included as a competitive inhibitor of scavenger receptor (SR-AI and SR-BI)-mediated lipid uptake (Acton et al., 1994). Uptake in the presence of maleyl-BSA was used as a measure of non-specific cell association of DiI. Untransfected cells were included as an additional negative control for background DiI-HDL and DiI-Ac-LDL uptake. To measure cell association of CT- B, cells were incubated with 5 μg/ml of alexa 488-CT-B and treated the same way as cells incubated with DiI labeled lipoproteins.

The accumulation of either DiI or alexa 488 fluorescence in cells was measured by flow cytometry. Figure 11 shows the results obtained for DiI-Ac-LDL uptake by CHO[*murine* SR-AI] cells (control) in a single representative experiment. Histograms of cell number versus fluorescence are plotted for untransfected CHO cells (top panel, black), CHO[*murine* SR-AI] cells (red) and CHO[*murine* SR-AI] cells incubated in the

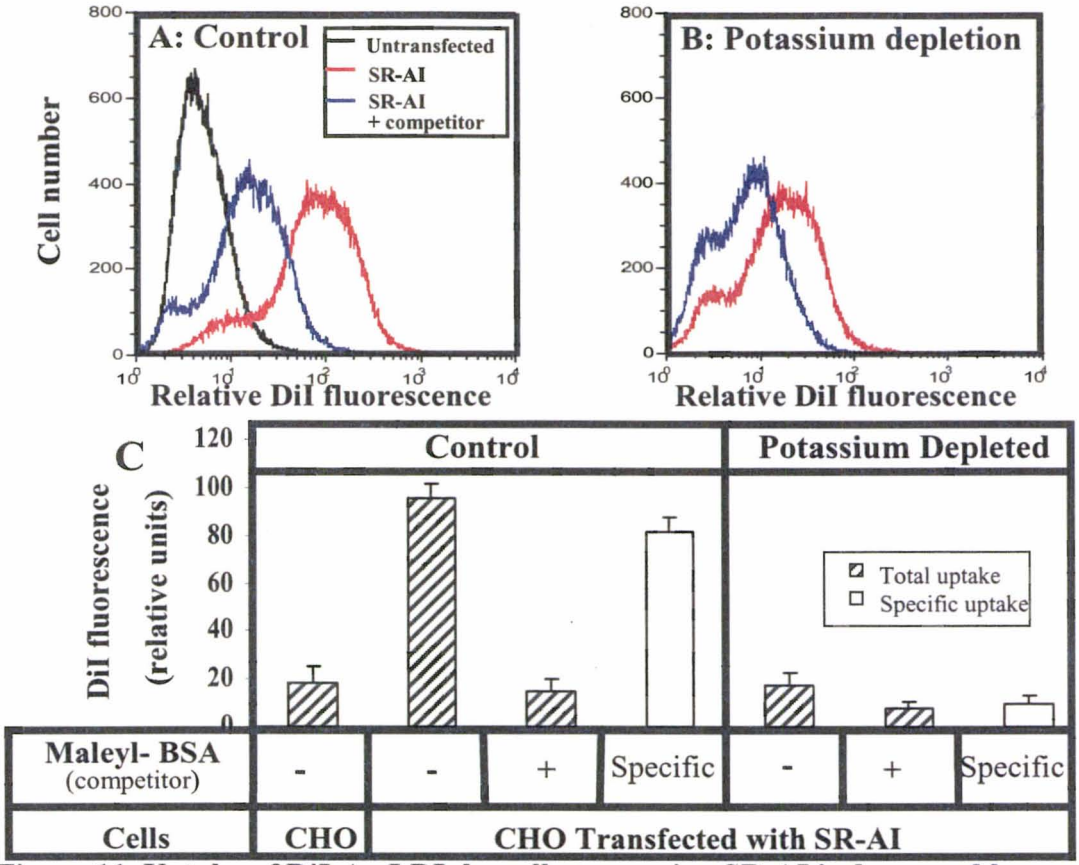

Figure 11. Uptake of DiI-Ac-LDL by cells expressing SR-AI is decreased by intracellular potassium depletion. Cells were grown ($5x10^4$ cells/$3.5cm^2$), in Ham's F12 containing 3%NCLPDS for two days. On day three, cells were washed with media (without additions), subjected to potassium depletion (*described in the Methods section 2.2.8*) and incubated with DiI-Ac-LDL for 2 hours at 37°C. DiI uptake was analyzed by flow cytometry using a FACScan instrument (FL2 channel emission 565-585 nm). Panel A shows histograms corresponding to control cells (no potassium depletion) and panel B shows histograms corresponding to potassium depleted cells. DiI-AcLDL uptake by untransfected CHO cells (black histogram in panel A) and CHO[mSR-AI] cells incubated with DiI-Ac-LDL without (red histogram in panels A and B) or with a 200 μg/ml concentration of maleyl-BSA (blue histograms.) Panels A and B correspond to a representative samples. The geometric mean of DiI fluorescence values, from three separate experiments involving duplicate samples was determined and the average values ± standard deviations are plotted in C. The left panel corresponds to control (untransfected) CHO cells, and the right panel corresponds to CHO[*murine* SR-AI] cells depleted of intracellular potassium. The difference between total uptake in the absence of competitor maleyl-BSA and uptake in the presence of 200 μg/ml maleyl-BSA was used as a measure of 'specific' uptake (open bars).

presence of maleyl-BSA (blue). DiI-accumulation in CHO[*murine* SR-AI] cells was greater (histogram shifted to the right) than in untransfected CHO cells. Maleyl-BSA decreased DiI-Ac-LDL uptake by CHO[*murine* SR-AI] cells (blue histogram shifted to left of the red one), as expected of a competitive inhibitor. In panel B, CHO[*murine* SR-AI] cells depleted of intracellular potassium, DiI-Ac-LDL uptake was decreased, represented by the histograms shifting to the lower fluorescence values relative to panel A), indicating that potassium depletion interfered with the mechanism of SR-AI mediated uptake of lipids from Ac-LDL.

For quantitative analysis of DiI uptake, the geometric mean of the histogram was taken as a measure of the average level of uptake for each cell population. To compare the results of independent experiments, the level of uptake by untreated transfected cells (in the case of Figure 11, panels A and B, of CHO[*murine* SR-AI] cells) was set as 100. The levels of uptake in transfected and untransfected cells treated with maleyl-BSA and/or potassium depletion were expressed relative to the value of 100. Panel C shows the average DiI-Ac-LDL uptake from three independent experiments. The left panel corresponds to CHO (untransfected) and CHO[*murine* SR-AI] cells that were not depleted of potassium (control cells) and the right panel shows uptake in potassium depleted cells. The level of DiI accumulation in cells in the presence of maleyl-BSA (non-specific uptake) was subtracted from that in absence of maleyl-BSA (total uptake) to determine the "specific" DiI uptake (unfilled bars in panel C). Depletion of intracellular potassium resulted in a substantial 88 % decrease in the specific DiI-Ac-LDL uptake by *murine* SR-AI.

We carried out similar analyses of both CT-B uptake by CHO cells and DiI uptake from DiI-Ac-LDL and DiI-HDL by stable cell lines over-expressing either *human* or mouse SR-BI. The results of these analyses are shown in Figure 12. Panel A shows the results of potassium depletion on DiI-Ac-LDL uptake by *murine* SR-AI from Figure 11. Panel B shows that potassium depletion also reduced CT-B uptake by CHO cells (note this is total uptake). Panel C shows *human* SR-BI mediated uptake of DiI, from DiI-HDL and DiI-Ac-LDL, in the presence (solid columns) and absence (open columns) of intracellular potassium. Potassium depletion inhibited *human* SR-BI mediated DiI uptake from both DiI-HDL and DiI-Ac-LDL. In contrast, depletion of potassium did not have a substantial effect on *murine* SR-BI dependent DiI uptake from DiI-HDL, whereas *murine* SR-BI mediated uptake of DiI from DiI-Ac-LDL was reduced by greater than 50%.

3.2.2. Effect of hyperosmolarity on SR-BI mediated lipid uptake from HDL and AcLDL

We carried out a similar analysis of the effects of exposing cells to hyperosmotic conditions, another treatment reported to block multiple endocytic pathways. Cells were incubated in media containing 0.4 M sucrose for 1 hr at 37°C, prior to incubation with either DiI-Ac-LDL, DiI-HDL or alexa 488 CT- B in the presence of 0.4 M sucrose. Control cells were incubated in iso-osmolar media containing 0.5% BSA *(Materials and Method 2.2.10. Lipid uptake assay in cells treated with hypertonic shock).*

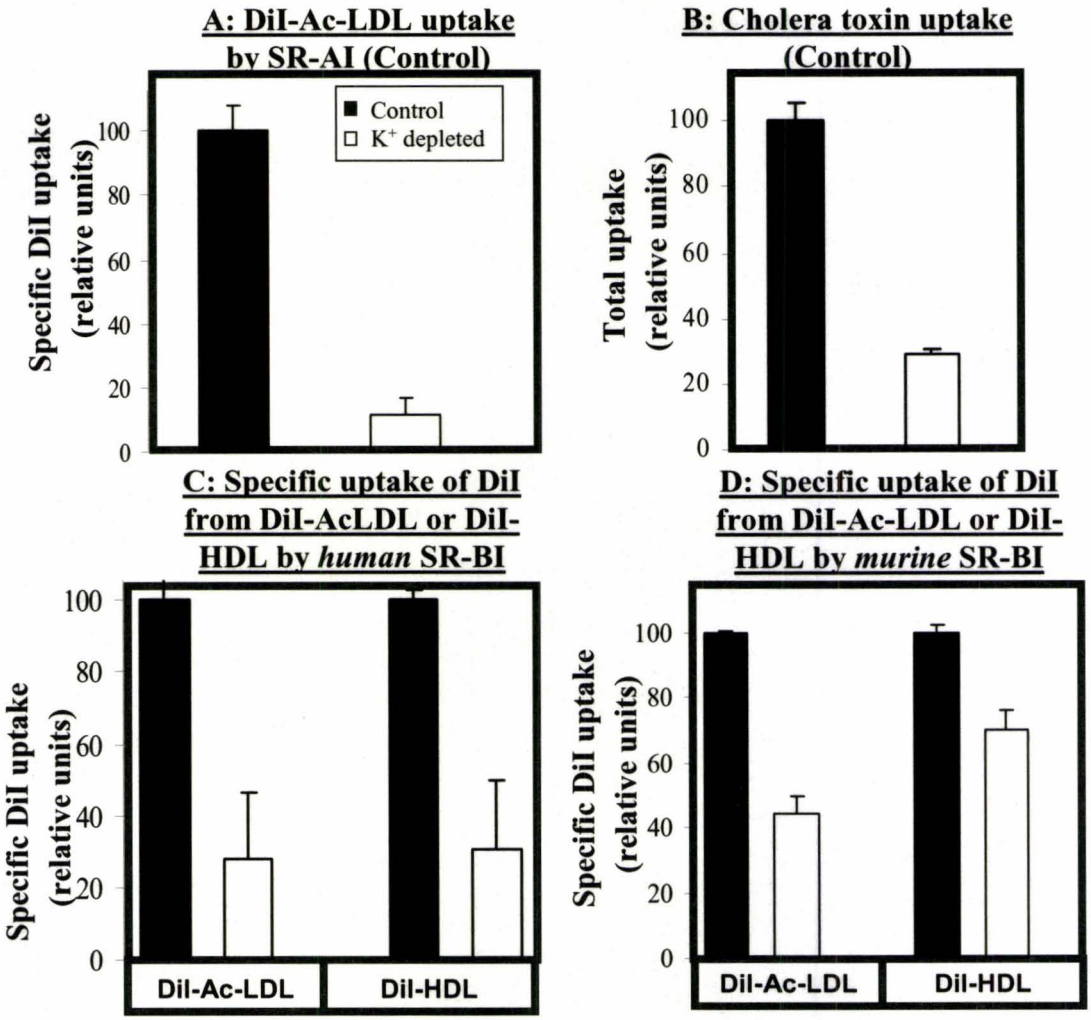

Figure 12: Effects of depletion of intracellular potassium on uptake of DiI from DiI-Ac-LDL or DiI-HDL by cells overexpressing either *human* or *murine* SR-BI.
Control CHO[*murine* SR-AI] (panel A), ldlA7 (panel B), ldlA[*human* SR-BI] (panel C) or ldlA[*murine* SR-BI] (panel D) cells were depleted of potassium (open bars) or mock treated (solid bars). Cells were either incubated with DiI-Ac-LDL or DiI-HDL (5 μg/ml), in the absence or presence of a 40-fold mass excess of maleyl-BSA competitor (200 mg/ml) (panels A, C and D) or alexa 488 labeled cholera toxin subunit B (CT-B; 5μg/ml) (panel B) for 2 hrs at 37°C as described in the legend to figure 11 (*details in section 3.2.1*). Cells were analyzed by flow cytometry as described in the legend to figure 11. The average DiI specific uptake (competible by maleyl-BSA, as described in fig 11) is plotted in panels A, C and D. Total uptake of CT-B is plotted in panel B. Values are expressed relative to control levels (set at 100). Data are the averages ± standard deviations of three independent experiments.

Figure 13 shows the effect of hyperosmolarity on specific uptake of DiI from DiI-Ac-LDL and DiI-HDL in ldlA[*murine* SR-BI] and ldlA[*human* SR-BI] cells (panels C and D). The effect of hyperosmolarity on DiI-Ac-LDL uptake by *murine* SR-AI and on CT-B uptake by CHO cells are shown in panels A and B. In the presence of hyperosmolar incubation conditions SR-AI mediated DiI-Ac-LDL uptake was reduced by 77 % but had no effect on CT-B uptake. Hyperosmolar incubation conditions inhibited *human* SR-BI mediated DiI uptake from both DiI-HDL and DiI-Ac-LDL (panel C). In contrast, hyperosmolar incubation conditions only inhibited *murine* SR-BI mediated DiI uptake from DiI-Ac-LDL (panel D, left), but not *murine* SR-BI mediated DiI uptake from DiI-HDL.

These results (summarized in Table 1) suggest that *human* SR-BI-mediated uptake of DiI from both DiI-HDL and DiI-Ac-LDL resembled SR-AI mediated uptake of DiI-Ac-LDL. Similarly, *murine* SR-BI mediated uptake of DiI from DiI-Ac-LDL also resembled DiI uptake from DiI-Ac-LDL mediated by SR-AI. In contrast *murine* SR-BI mediated uptake of DiI from DiI-HDL did not resemble SR-AI mediated DiI-Ac-LDL uptake, but in the presence of hyperosmolar sucrose concentration, behaved like CT-B uptake.

3.3. Co-localization of mRFP-*human*-SR-BI with EGFP-Clathrin

Previous research has demonstrated that *murine* SR-BI partially co-localized with caveolin-1 in a low density sub-fraction of plasma membranes in a number of cell types, including CHO cells (Babitt et al., 1997). That study also showed that by

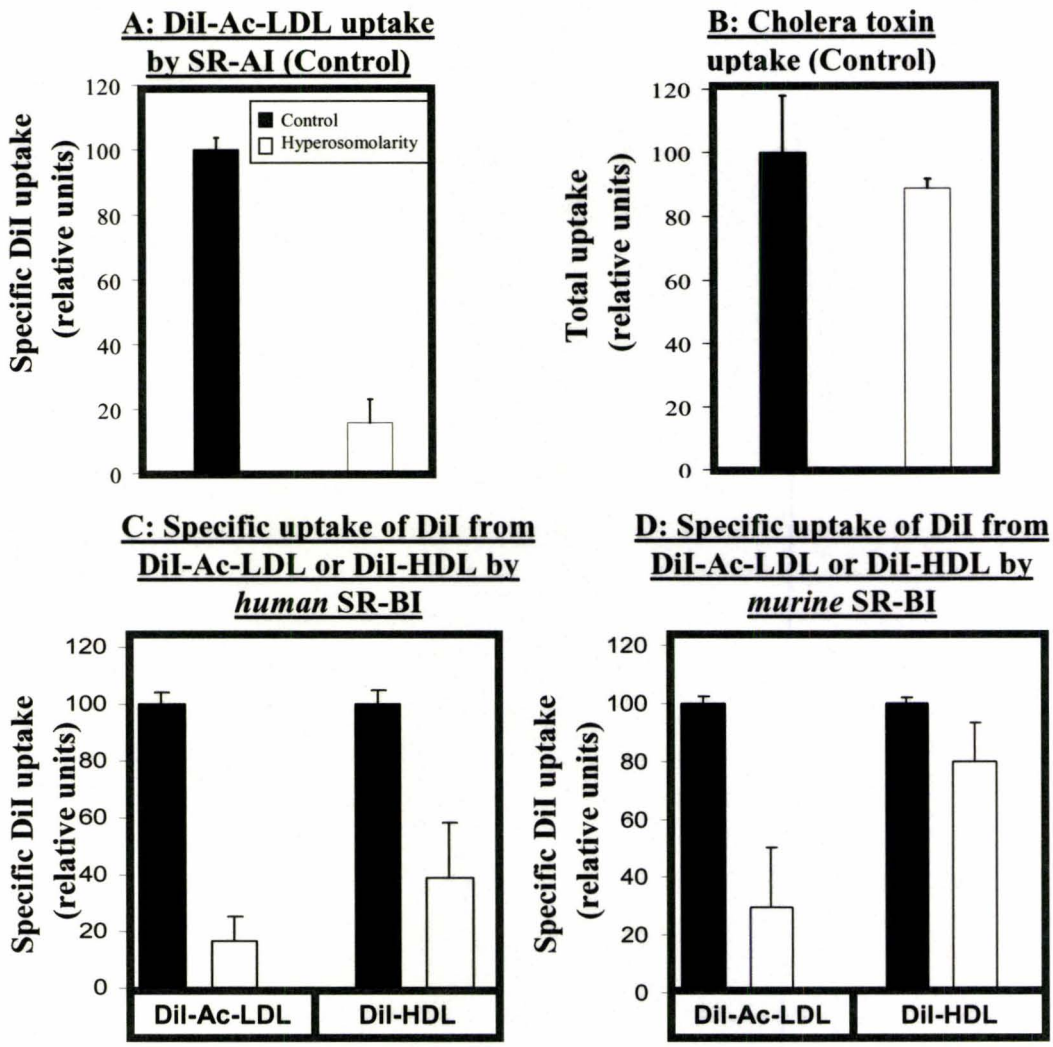

Figure 13: Effects of hyperosmotic treatment on uptake of DiI from DiI-Ac-LDL or DiI-HDL by cells overexpressing either *human* or *murine* SR-BI. Control CHO[*murine* SR-AI] (panel A), ldlA7 (panel B), ldlA[*human* SR-BI] (panel C) or ldlA[*murine*SR-BI] (panel D) cells were incubated in medium containing 0.4 M sucrose (hyperosmotic solution, open bars) or 0.5% BSA (control, solid bars) prior to and during incubation with either DiI-Ac-LDL, DiI-HDL or alexa 488-CT-B and flow cytometric analysis as described in the legends to figures 11 and 12 and in section 3.2.2. The average DiI specific uptake (competible by maleyl BSA) is plotted in panels A, C and D. Total uptake of CT-B is plotted in panel B. Values are expressed relative to control levels (set at 100). Data are the averages ± standard deviations of three independent experiments.

Table1: Effect of intracellular potassium depletion and hyperosmolarity on DiI uptake from DiIAcLDL and DiIHDL, by SR-BI.

Receptor	Ligands	DiI uptake (percent of untreated cells)	
		*Potassium depletion	**Hyperosmolar sucrose
Ganglioside GM1	Cholera toxin subunit B	29 ±2%	88 ±3%
SR-AI	DiIAcLDL	12 ± 4%	16 ± 8%
mSR-BI	DiIAcLDL	44 ± 11%	30 ± 20%
	DiIHDL	*70 ± 5%	*80 ± 14%
hSR-BI	DiIAcLDL	28 ± 15%	17 ± 8%
	DiIHDL	30 ± 15%	39 ±20%

$p < 0.032$ for all values except * ($p > 0.10$)

immunofluorescence microscopy SR-BI did not co-localize with clathrin (Babitt et al., 1997). However, that study was done in the absence of added lipoproteins in the medium. To determine if the two proteins co-localize in the presence of HDL or Ac-LDL in the medium, colocalization studies were done in cells stably co-expressing mRFP-*human*-SR-BI and EGFP tagged clathrin (light chain) in ldlA7 cells.

Stable cell lines expressing mRFP-*human*-SR-BI, EGFP-clathrin or both mRFP-*human*-SR-BI and EGFP-clathrin were generated *(Materials and Method 2.2.5.3).* Others have shown that EGFP tag does not to interfere with the sub cellular localization of clathrin (Mueller et al., 2004). LdlA[mRFP-*human*-SR-BI+EGFP-clathrin] cells were cultured on glass cover slips and incubated with 5 μg/ml of either Ac-LDL or HDL, or incubation medium without lipoproteins for 2 hr at 37 °C. Cells were then washed and fixed with 2.5% paraformaldehyde for 30 minutes at room temperature. Fixed cells were imaged by laser confocal microscopy using a 63x water immersion objective (Figure 14).

Control cells for this experiment included cells expressing either EGFP-clathrin or mRFP-*human*-SR-BI alone, to ensure that EGFP fluorescence was not detected in the red channel and mRFP fluorescence was not detected in the green channel (not shown). Panels A, D and G show the distribution of mRFP-*human*-SR-BI (red fluorescence), panels B, E and H show the distribution of EGFP-clathrin (green fluorescence) and panel C, F and I show the merged images of mRFP-*human*-SR-BI and EGFP-clathrin in the same cells. No co-localization of mRFP-*human*-SR-BI and EGFP-clathrin was observed in the absence (panels A-C), or presence of lipoproteins ligands *1)* HDL (panels D-F) or *2)* of Ac-LDL (panels G-I). These results are consistent with what was previously

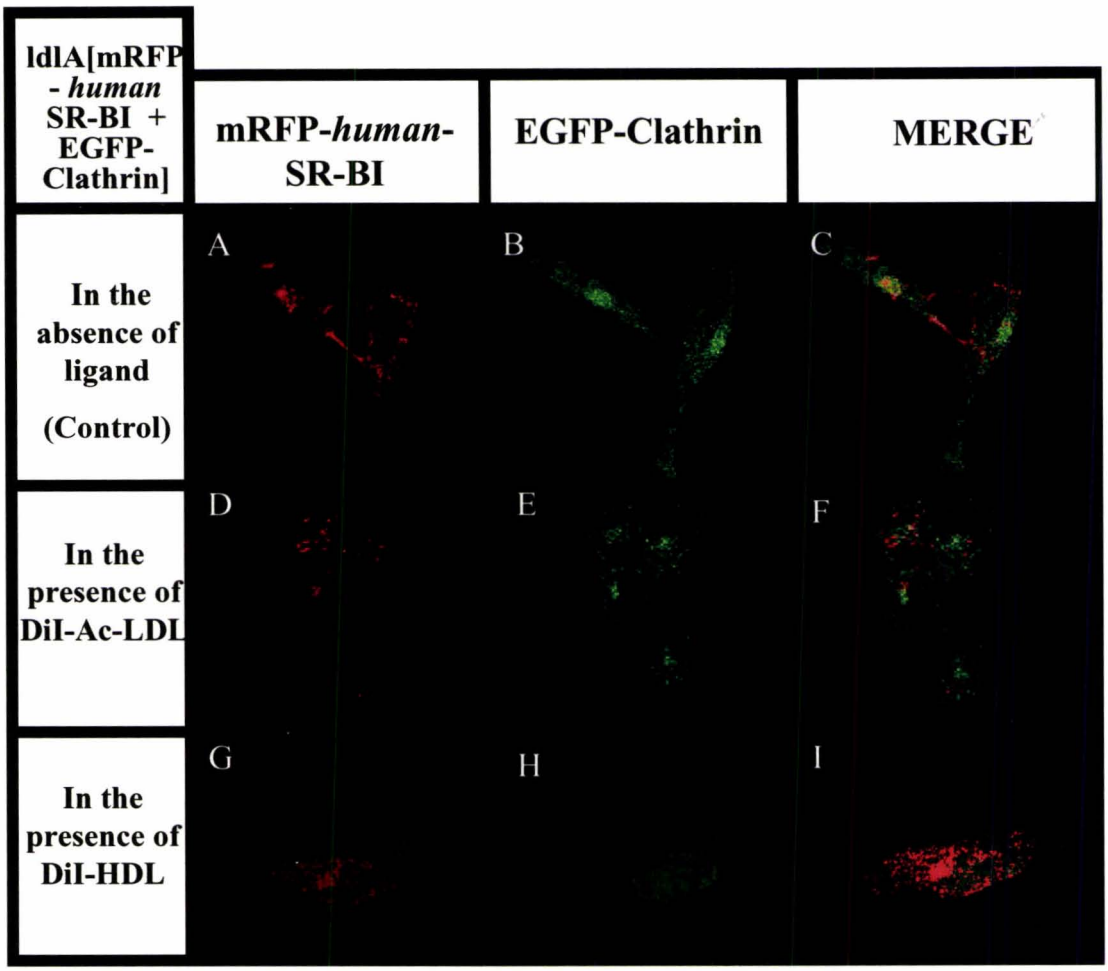

Figure 14: mRFP- *human*SR-BI does not colocalize with EGFP- clathrin in cells. LdlA[EGFP-Clathrin + mRFP-*human*-SR-BI] cells were seeded on glass bottom dishes, in growth media containing 3% lipoprotein deficient serum (NCLPDS). On day three, cells were incubated with medium in the absence of lipoprotein ligands (top row; panels A-C), or in the presence of Ac-LDL (second row; panels D-F) or HDL (bottom row; panels G-I) for two hours at 37°C. Cells were washed and fixed in 2.5% paraformaldehyde. mRFP fluorescence ("Red"; panels A, D and G), EGFP fluorescence ("Green"; panels B, E and H) were visualized using a Zeiss laser confocal microscope with a 63x water immersion objective. Panels C, F and I show the merged images.

reported for *murine* SR-BI in the absence of ligands (Babitt et al., 1997). These data suggest that *human* SR-BI mediated uptake of Ac-LDL or HDL does not occur via clathrin coated pits.

3.4. Role of dynamin in SR-BI mediated lipid uptake from lipoproteins

Fission of endocytic vesicles from the plasma membrane is dependent on dynamins. Over-expression of a dominant negative mutant dynamin 1 (Dyn1-K44A) has been shown to disrupt fission of endocytic vesicles from the plasma membrane, interrupting a variety of different endocytic pathways, including clathrin, and caveolae mediated endocytosis (Sever et al., 2000; Henley et al., 1998).

3.4.1. Dyn1-K44A expression in cells

Overexpression of Dyn1K44A is suspected to be toxic in some cell types (Altschuler et al., 1998). We therefore expressed Dyn1K44A in transiently transfected ldlA7 cells that had been cultured in the presence of 3% NCLPDS for one day. The next day cells were transfected with a plasmid encoding hemaglutinin (HA) epitope-tagged Dyn1-K44A (pHA-Dyn1-K44A). Cells were harvested 16, 24 and 48 hr later and the expression of HA-tagged Dyn1K44A was determined by immunoblotting with an anti-HA antibody. In Figure 15, equal amounts of total cell protein were loaded in each lane. No band was seen in lysates from mock transfected cells (lane 1). An approximately 100 kDa band was detected in lysates from cells prepared 16, 24 and 48 hr after transfection (lanes 2-4). Maximum expression of HA-Dyn1-K44A appeared by 16 hr after transfection.

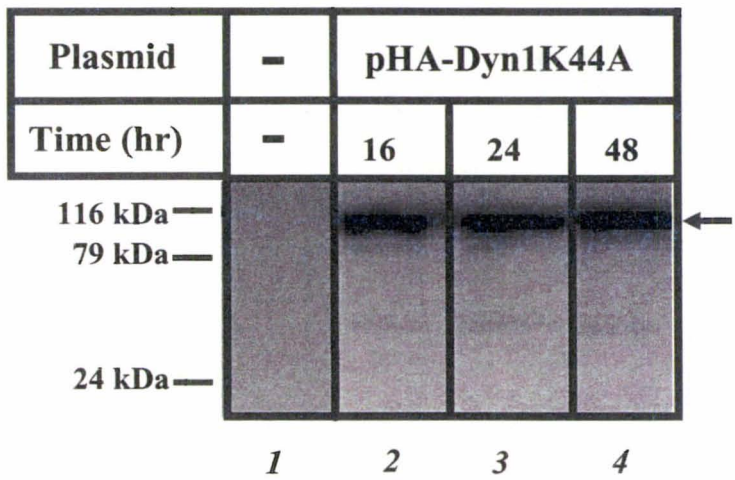

Figure 15: Immunoblot analysis of HA- tagged dynamin1 K44A expression in transfected ldlA7 cells. LdlA7 cells were transfected without DNA (mock; lane 2), or with pHA-Dyn1 K44A (lanes 3-5). Cells were harvested 16, 24 and 48 hrs post transfection (lanes 3, 4 and 5 respectively). Cell lysates were subjected to SDS PAGE, using a 10% polyacrylamide separating gel and proteins were electrophoretically transferred to PVDF. Immunoblotting with a rabbit an anti-HA antibody (Santa Cruz Biotechnology, CA) and an HRP conjugated anti-rabbit secondary antibody was performed (*described in section 2.2.12.3.*)

The expression of HA tagged Dyn1-K44A in permeabilized transfected cells was determined by immunofluorescence using the rabbit anti-HA antibody and the alexa 488-labeled anti-rabbit secondary antibody. Cells were transfected with both the pHA-Dyn1-K44A and pmRFP-*human*-SR-BI plasmids (9:1 ratio). Cells were fixed with 2.5% formaldehyde, permeablized with 1% triton-X 100 and labeled with the anti-HA primary and alexa 488 secondary antibodies. Nuclei were stained with DAPI (300nM in PBS) for 5 min at room temperature. Many cells died post-transfection, resulting in apparently low transfection efficiency (which was expected of a dominant negative mutant and from the results obtained from Immunoblotting experiments). Fluorescence was visualized using Zeiss Axiovert fluorescence microscope using Zeiss filter set 13 for alexa 488 (Dyn1-K44A, panel A), filter set 10 for mRFP-*human*-SR-BI (panel B) and filter set 01 for DAPI (panel C). Control single labeled cells were included to ensure that green and red fluorescence were only detected with the appropriate filters. All of the cells expressing green fluorescence also expressed red fluorescence (see panel D). Therefore a fluorescent marker protein could be used as an accurate reporter of Dyn1-K44A expression in cells. Perhaps surprisingly, we did not see evidence of co-localization of mRFP- *human*SR-BI with HA-tagged Dyn1K44A. Further experiments (e.g. distribution in the presence of lipoproteins, the use of fluorescent protein tagged Dyn for live cell imaging and the use of wild type rather than mutant Dyn1) will have to be performed to address this question. The results of Figure 16 do demonstrate, however, that co-transfection with pDyn1K44A and a plasmid expressing a fluorescent protein is a reliable method of marking transfected

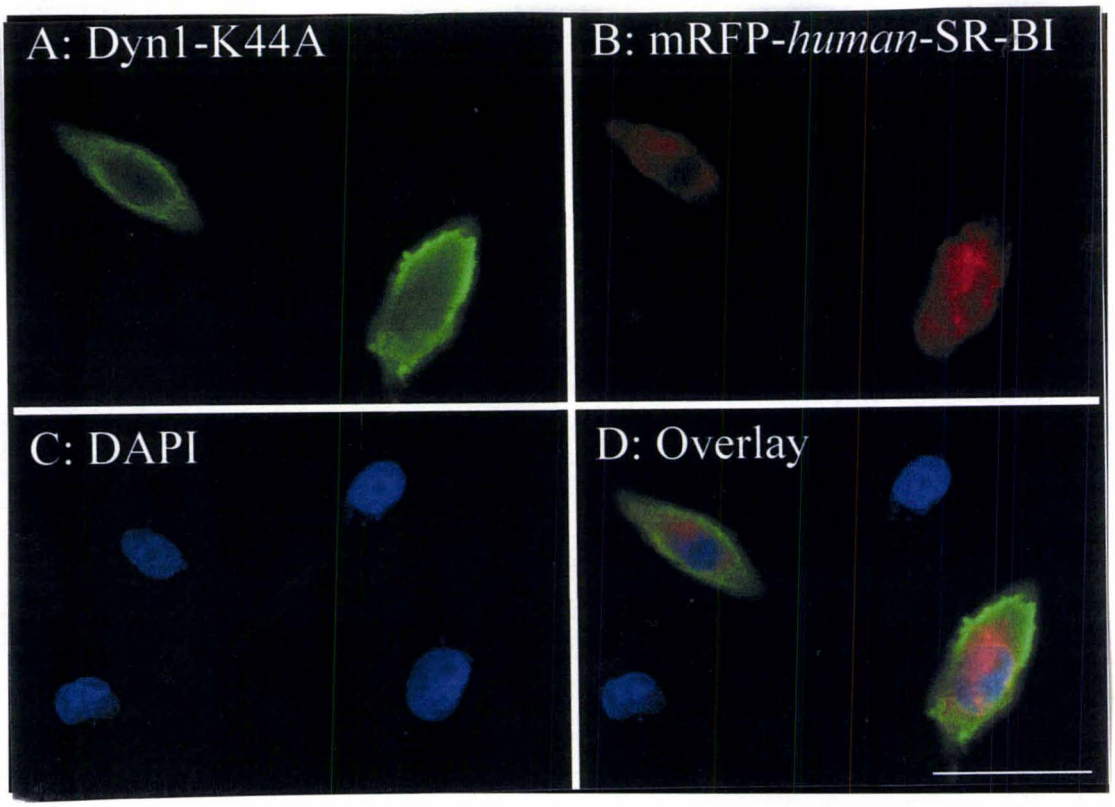

Figure 16. Co-expression of HA-tagged dynamin 1 K44A and mRFP-*human*-SR-BI in transfected cells: Cells were grown on poly D-lysine-coated glass bottom plates in 2 ml of medium containing 3% NCLPDS. Cells were co-transfected with pHA-Dyn1 K44A and pmRFP-*human*-SR-BI. Sixteen hours post-transfection, cells were washed fixed in 2.5% paraformaldehyde, permeabilized with 0.1 % Triton X-100 and subjected to immunofluorescence microscopy using a rabbit anti-HA antibody and an alexa 488 anti-rabbit secondary antibody (*described in the Methods section 2.2.13*). After immunofluorescence, cells were incubated with 300nM DAPI in PBS for 5 minutes to stain cell nuclei. Cells were imaged using a Zeiss Axiovert 200M fluorescence microscope with Zeiss filter sets 13 (for Alexa 488; panel A), 10 (for mRFP fluorescence; panel B) and filter set 01 (for DAPI fluorescence; panel C). The overlayed images are shown in panel D. (Scale bar = 20 μm)

cells harboring the pDyn1K44A plasmid. We made use of this finding in the following experiment.

3.4.2. Dyn1-K44A expression decreased DiI uptake in cells

To test the effect of Dyn1-K44A expression on SR-BI mediated DiI uptake, we measured DiI uptake from either DiI-Ac-LDL or DiI-HDL by CHO[*murine SR-AI*], ldlA[*human* SR-BI] and ldlA[*murine* SR-BI] cells that had been transfected with pHA-Dyn1-K44A and pEGFP (to mark transfected cells; 9:1 ratio of plasmids respectively). Control cells were transfected with pEGFP and a plasmid expressing the neomycin resistance gene (pSVNeo) to balance the plasmid load. Dyn1-K44A transfected and control cells were incubated (16 hr post transfection) with 5 μg/ml of DiI-Ac-LDL or DiI-HDL for 2 hr at 37 °C. Cells were washed and imaged using an inverted fluorescence microscope at 40x magnification. EGFP fluorescence was detected using Zeiss filter set 13, DiI fluorescence was detected using Zeiss filter set 10. Controls were included to verify that no crossover of fluorescence between the channels was detected (not shown).

Figure 17 shows representative images of ldlA[*human* SR-BI] cells transfected with either control pSVNeo and pEGFP (A-F) or pHA-Dyn1-K44A and pEGFP (G-L). Cells were incubated with either DiI-Ac-LDL (B and J) or DiI-HDL (E and K). The EGFP fluorescence images (panels A, D, G and J) were used to identify transfected cells and to trace periphery of these cells. The trace was then overlayed onto the corresponding DiI fluorescence images of the same cells (panels B, E, H and K show DiI fluorescence images and C, F, I and L show images with traces overlayed). Simple PCI software was

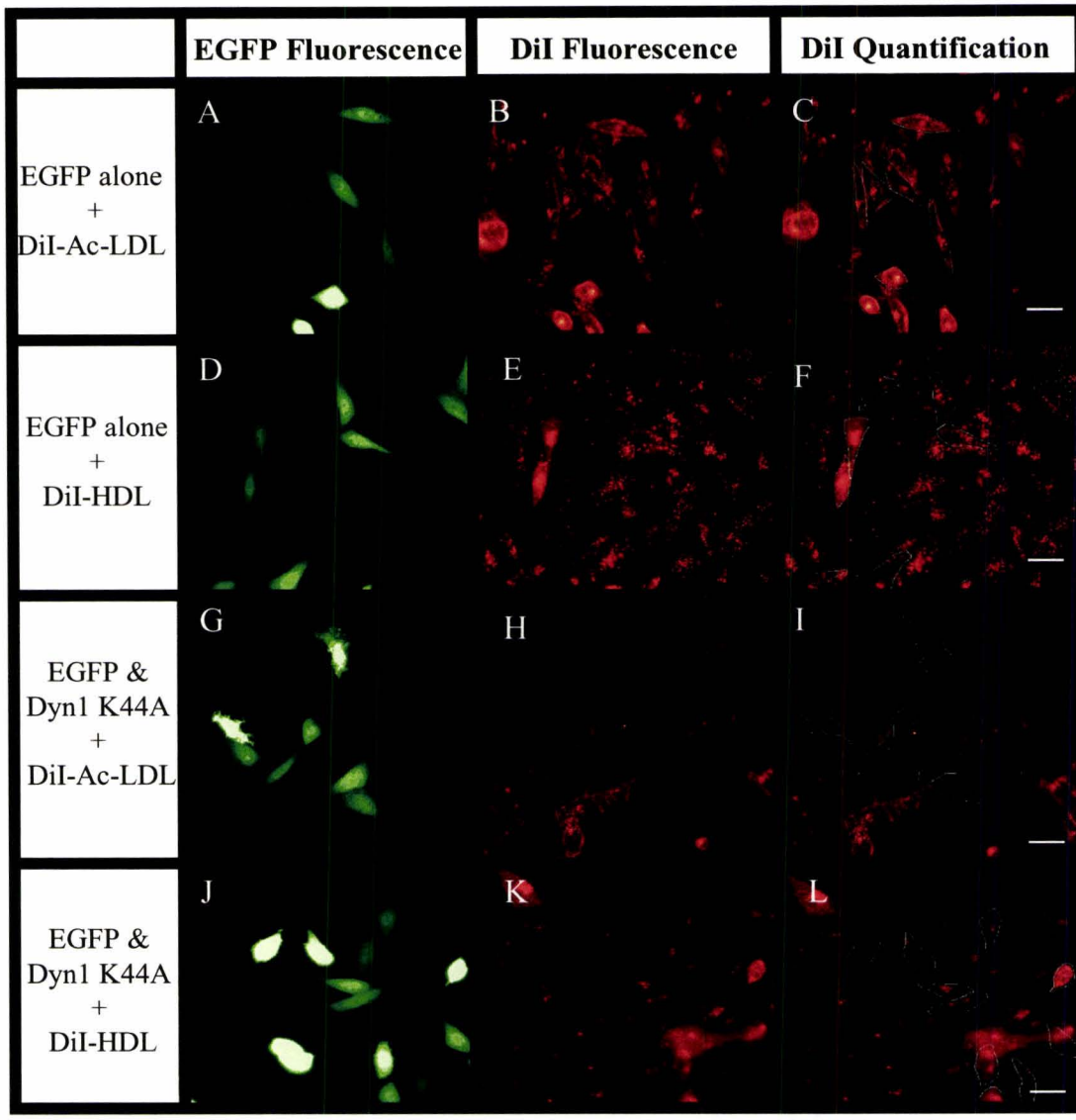

Figure 17: Effect of dominant negative dynamin 1 (Dyn1K44A) on *human* SR-BI mediated DiI uptake from DiI-Ac-LDL and DiI-HDL: LdlA[*human* SR-BI] cells seeded on glass bottom dishes, were transfected with pEGFP-C1 (encoding EGFP) and a control plasmid (pSVNeo) (panels A-F), or pEGFP-C1 and pHA-Dyn1-K44A. Sixteen hours post transfection, cells were incubated with 5 µg/ml of either DiI-Ac-LDL or DiI-HDL for 2 hrs at 37 °C. Cells were imaged using Zeiss Axiovert 200 M microscope with filter sets 13 (EGFP fluorescence; panels A, D, G and J) and 10 (DiI fluorescence; panels B, E, H and K). The boundaries of transfected cells (EGFP expressing) were determined from the EGFP fluorescent images and were overlayed on the corresponding DiI-fluorescence images (panels C, F, I, and L). Simple PCI software was used to determine the intensity of DiI fluorescence within the identified transfected cells.

used to quantify DiI fluorescence from these images within the boundaries (method from the theses of Jill Taylor, and Stewart Irwin).

The average DiI fluorescence in control cells and cells expressing Dyn1-K44A was calculated for CHO[*murine SR-AI*] cells, ldlA[*human* SR-BI] cells and ldlA[*murine* SR-BI] cells. Data is plotted in Figure 18. It appears that in CHO[*murine SR-AI*] cells (A), ldlA[*human* SR-BI] cells (B) and ldlA[*murine* SR-BI] (C) Dyn1-K44A over-expression resulted in an approximately 30 percent reduction in DiI uptake from either DiI-Ac-LDL or DiI-HDL, compared to the mock transfected cells. Percent inhibition is tabulated in Table 2. A similar magnitude of the decreases in DiI uptake from either DiI-HDL or Ac-LDL mediated by both *human* and mouse SR-BI and the decrease in *murine* SR-AI mediated DiI-Ac-LDL uptake indicates that dynamin dependent fission of endocytic vesicles has a role in SR-BI mediated uptake of lipid from both lipoproteins.

3.5. Role of microfilaments in SR-BI mediated lipid uptake from HDL and AcLDL

Actin microfilaments are involved in early events in endocytosis, including the internalization and movement of endocytic vesicles from the cell membrane (Durrbach et al., 1996; Mundy et al., 2002; Qualmann et al., 2000). To establish the role of microfilament in SR-BI mediated lipid uptake from lipoproteins we used cytochalasin D, which disrupts microfilament by inhibiting actin cross linking and polymerization (Goddette and Frieden, 1986). We measured DiI uptake from DiI-Ac-LDL by CHO[*murine* SR-AI] cells (control for clathrin mediated endocytosis) and from DiI-HDL or DiI-Ac-LDL by ldlA[*human* SR-BI] and ldlA[*murine* SR-BI] cells. Cells were

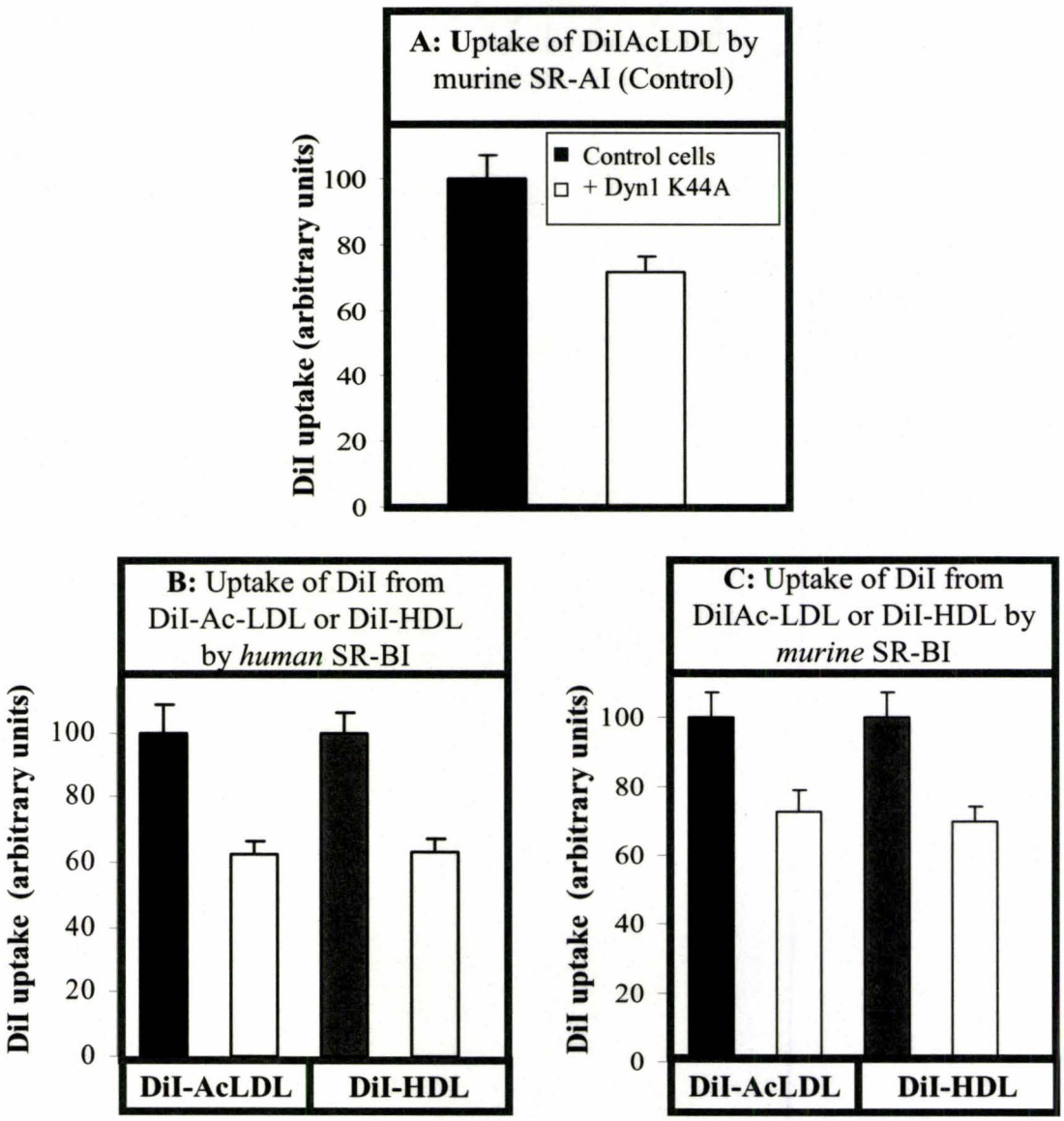

Figure 18: Effect of Dyn1 K44A expression on by *human* and *murine* SR-BI mediated DiI uptake fom DiI-Ac-LDL or DiI-HDL. CHO[*murine* SR-AI] (panel A), ldlA[*human* SR-BI] (panel B) or ldlA[*murine* SR-BI] (panel C) cells were transfected with pEGFP-C1 (open bars) or pEGFP-C1 and pHA-Dyn1-K44A (solid bars.) Cells were transfected, assayed and imaged as described in the legend of figure 17. Simple PCI software was used to quantify the DiI fluorescence expressing EGFP (marker for transfection.) Reported here is the mean DiI fluorescence values in samples of cells (n<98), error bars indicate the value of standard error.

either treated with or without cytochalasin D (10 µg/ml) *(Materials and Method 2.2.11. Treatment of cells with cytochalasin D or colchicine).*

Treatment of CHO[*murine SR-AI*] cells with cytochalasin D reduced DiI-Ac-LDL uptake by approximately 50 % (Figure 19, panel A). Similarly, cytochalasin D treatment of ldlA[*human* SR-BI] cells inhibited DiI uptake from DiI-Ac-LDL and DiI-HDL by 64 and 34 % respectively (panel B). Cytochalasin D also inhibited DiI uptake from DiI-Ac-LDL in ldlA[*murine* SR-BI] cells by 54%. In contrast, DiI uptake from DiI-HDL was not affected in ldlA[*murine* SR-BI] cells (panel C). This data was reminiscent of that obtained when cells were depleted of intracellular potassium or incubated in hyperosmolar solution (Figures 12 and 13, or table 1).

To observe the effect of cytochalasin D on the dynamics of SR-BI mediated lipid uptake, CHO[*murine* SR-AI], ldlA[*murine* SR-BI] and ldlA[*human* SR-BI] were incubated with DiI-Ac-LDL or DiI-HDL in the presence or absence of cytochalasin D, and observed by live fluorescence microscopy at the temperature permissive for endocytosis (37°C) *(Materials and Method 2.2.12.4).* Imaging of control cells (not treated with cytochalasin D) revealed that DiI derived from DiI-HDL and DiI-Ac-LDL was concentrated in discrete spherical structures, which displayed a variety of motions in the cell (rapid, slow, long range, short range, vertical and horizontal). These vesicles resembled endocytic vesicles due to their size, shape and range of movement in the cell. Cell treated with cytochalasin D had distinctive change in cellular morphology (as seen in data previously published by others (Fujimoto et al., 2000)). In the presence of the drug, cell had a dome like appearance in the middle, from which flat filamentous projections

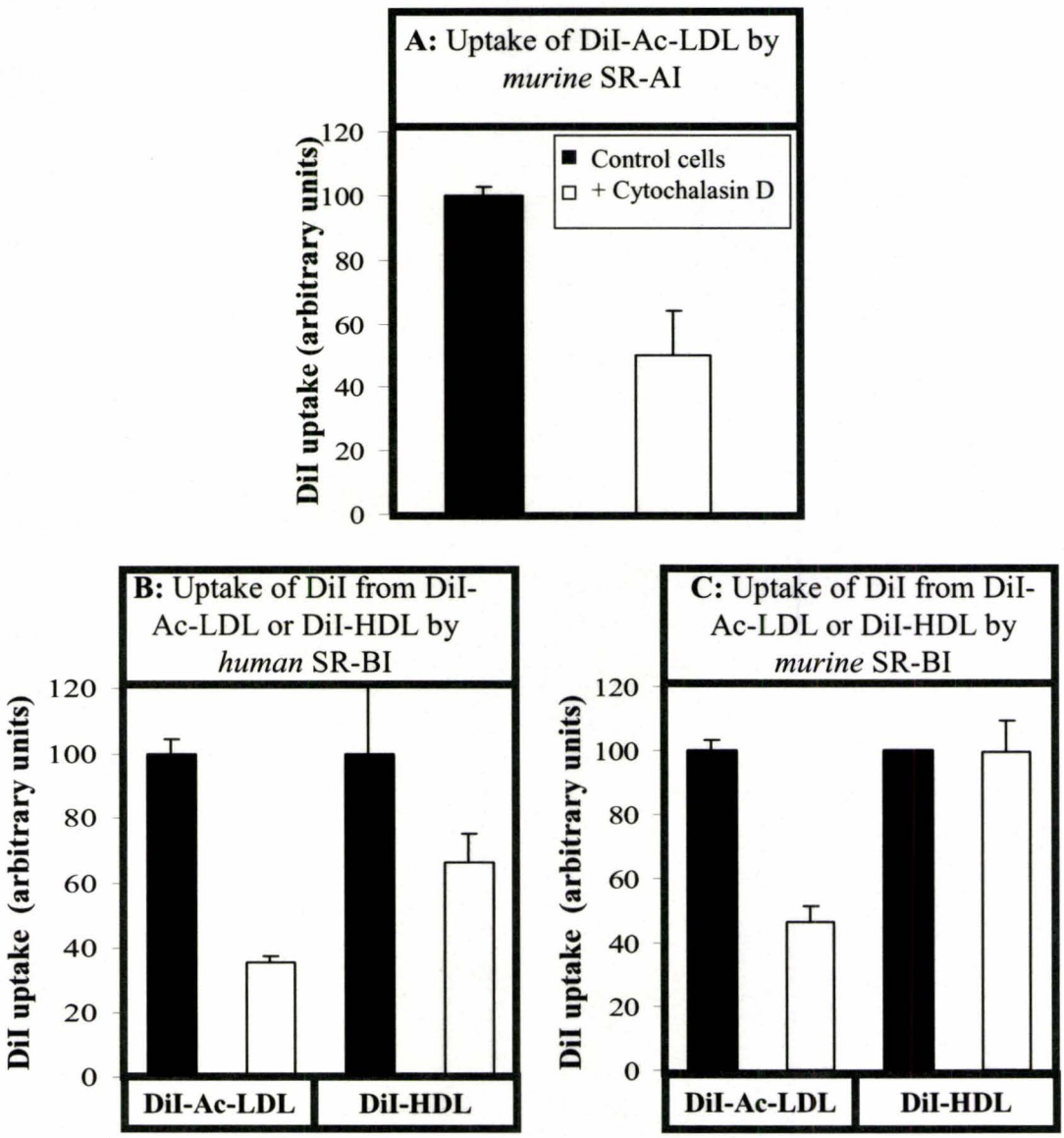

Figure 19: Effect of cytochalasin D on uptake of DiI from DiI-Ac-LDL or DiI-HDL by *human* and *murine* SR-BI. Control CHO[*murine* SR-AI] (panel A), ldlA[*human* SR-BI] (panel B) or ldlA[*murine* SR-BI] (panel C) cells were cultured in media containing 3 % NCLPDS for two days. On day three, control cells were treated with (open bars) or without (solid bars) 10 μM cytochalasin D in media containing 0.5 % BSA for 2 hrs prior to and during incubation with DiI-Ac-LDL or DiI-HDL (each 5 μg/ml) at 37°C and subsequent flow cytometric analysis (*as described in section 2.2.12.2*). Average DiI uptake values are expressed relative to control levels (set at 100).

extended outwards. It appears that Cytochalasin D might have had a slight effect on the movement of vesicles; but more quantitative methods would have to be used to substantiate that. Live cell imaging of cells under the fluorescence microscope, showing vesicular dynamics is included as AVI files on the CD (supplementary data).

In order to study the dynamic interaction of DiI derived lipid and SR-BI, we repeated the above experiment, using cell line expressing EGFP-tagged *human* SR-BI (ldlA[EGFP-*human*-SR-BI] cells). Cells were incubated with or without cytochalasin D. In control cells, EGFP-*human*-SR-BI and DiI fluorescence was concentrated in dynamic vesicles distributed throughout the cell, and in the areas of cell-cell contact as described above. The vesicles containing DiI lipid and EGFP-*human* SR-BI exhibited short range motion as well as rapid and long range three dimensional movements within the cells. An accumulation of fluorescence in the perinuclear region of the cell was observed. Both EGFP-*human*-SR-BI and DiI fluorescence was concentrated on areas of cell-cell contact; that was also the area of the cell where there was an increased co-localization of DiI and EGFP-*human*-SR-BI. DiI lipid from DiI-Ac-LDL appeared to be mostly on the cell periphery, whereas DiI lipid from DiI-HDL seemed to be localized mostly into vesicles inside the cell.

In cells treated with cytochalasin D, there was an increase in DiI co-localized with EGFP-*human* SR-BI either on or near the cell surface. Vesicles containing both DiI and EGFP-*human* SR-BI appear to be less dynamic than those not treated with cytochalasin D. Figure 20 shows static images of ldlA[EGFP-*human* SR-BI] cells incubated with DiI-Ac-LDL or DiI-HDL in the absence (A and D) or presence of cytochalasin D (B and E).

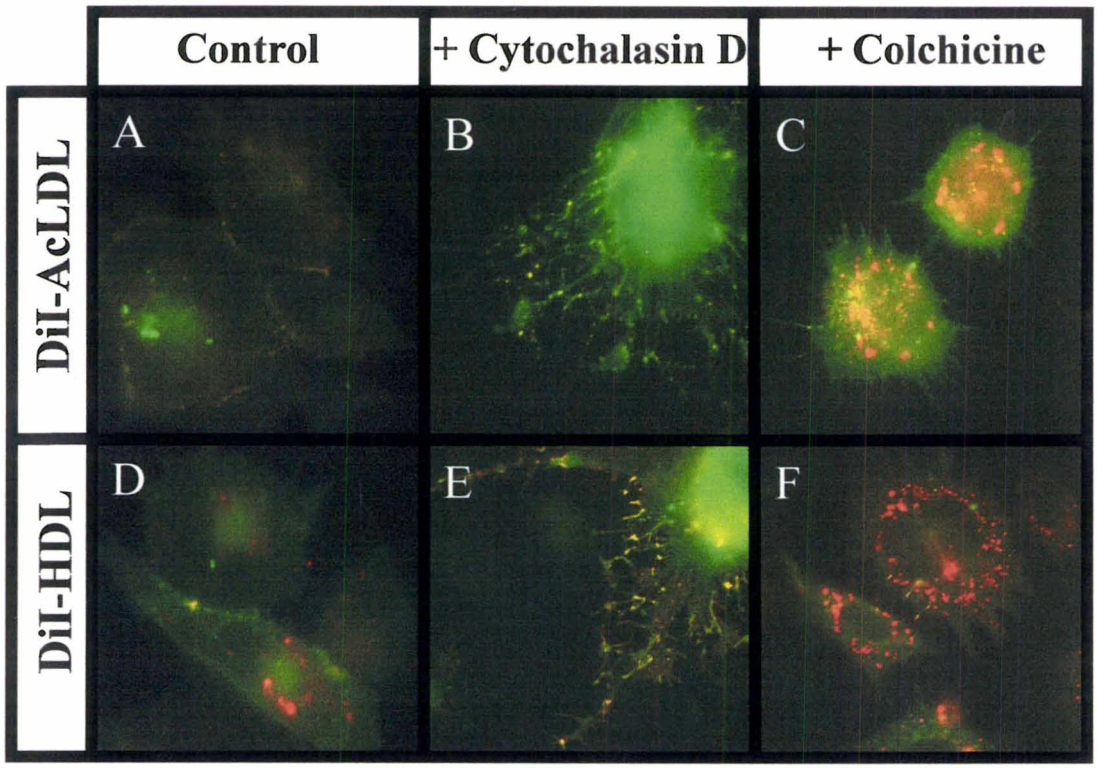

Figure 20. Effects of cytochalasin D and colchicine on the distribution of *human* SR-BI and lipoprotein derived DiI in transfected cells: ldlA[EGFP-*human*-SR-BI] cells were plated on glass bottom dishes and cultured for two days as described in the legends to figure 17. Untreated cells (panels A and D) and cells treated with 10 mM of either cytochalasin D (panels B and E) colchicine (panels C and F) 2 hrs prior to and during the 2 hrs incubation at 37 °C with either DiI-Ac-LDL (panels A-C) or DiI-HDL (panels D-F) (5 μg/ml) (*details in section 2.2.10)* were imaged live at 37°C in the continued absence or presence of drugs. EGFP (green) and DiI fluorescence (red) images, captured using separate filter sets, were merged (C and F.) Representative images are shown.

3.6. Role of microtubules in SR-BI mediated lipid uptake from HDL and AcLDL

Microtubules serve as tracks for long range, rapid movements of transport intermediates between compartments in the secretory and the endocytic pathways (Mundy et al., 2002; Osland et al., 1979). To determine whether the movement of DiI carrying vesicles requires microtubules, the effect of treating cells with colchicine on DiI uptake and distribution in cells was determined. Colchicine has been shown to disrupt polymerization of α-tubulin and β-tubulin, which results in disruption of microtubular structure, and therefore their function in cells (Durrbach et al., 1996; Osland et al., 1979).

CHO[*murine* SR-AI], ldlA[*murine* SR-BI] and ldlA[*human* SR-BI] cells were incubated with 5 μg/ml of DiI-HDL and DiI-Ac-LDL, in the presence or absence of 10 μM colchicine *(Materials and Method 2.2.11 Treatment of cells with cytochalasin D or colchicine).* Live adherent cells were imaged using a fluorescence microscope at 37°C (permissive for vesicular movement). Treatment of CHO[*murine* SR-AI], ldlA[*murine* SR-BI] and ldlA[*human* SR-BI] cells with colchicine appeared to impair the long range movement of the dynamic DiI-stained vesicular structures in observed in control cells (*described in section 3.5).* Note that some localized movement, possibly attributed to Brownian motion was still observed. Furthermore, the DiI stained vesicle like structures in colchicine treated cells appear to be larger in diameter, compared to the control (untreated) cells. This data suggests that microtubules play a role in movement of DiI containing vesicles, and the trafficking of lipoprotein derived lipid within the cell. Live cell imaging of cells under the fluorescence microscope, showing vesicular dynamics is included as AVI files on the CD (supplementary data).

Once again, to study the effect of colchicine on the dynamics of interaction between SR-BI and lipoprotein derived DiI lipid in cells, we repeated the above experiment using ldlA[EGFP-*human* SR-BI] cells. It was observed that as described previously, SR-BI containing vesicles (green) and DiI containing vesicles (red) were dynamic. Often, SR-BI and DiI were present in the same vesicular structure (yellow). In the presence of colchicine, vesicles containing EGFP-*human*-SR-BI or DiI became static and larger in size compared to vesicles in untreated cells. Moreover, in cells treated with colchicine, there was an increase in co-localization of EGFP-*human*-SR-BI and DiI compared to untreated cells.

To determine whether the microtubule dependent dynamics of SR-BI containing vesicles or DiI-containing vesicles was required for DiI uptake, we measured DiI uptake from DiI-HDL or DiI-Ac-LDL in ldlA[*murine* SR-BI] or ldlA[*human* SR-BI] cells treated with or without colchicine. CHO[*murine* SR-AI] cells were used as controls for colchicine treatment. Cells were analyzed using a flow cytometer. Figure 21 shows DiI accumulation in CHO[*murine* SR-AI] cells incubated with DiI-Ac-LDL (panel A), ldlA[*human* SR-BI] cells incubated with either DiI-Ac-LDL or DiI-HDL (panel B) and ldlA[*murine* SR-BI] cells incubated with either DiI-Ac-LDL or DiI-HDL (panel C), in the absence (solid bars) or presence (open bars)of colchicine. Colchicine treatment resulted in a slight, but not statistically significant decrease in DiI uptake from DiI-Ac-LDL by CHO[*murine* SR-AI] cells and from DiI-Ac-LDL and DiI-HDL by ldlA[*human* SR-BI] cells. *Murine* SR-BI mediated uptake of DiI from either DiI-Ac-LDL or DiI-HDL was not affected by colchicine (panel C).

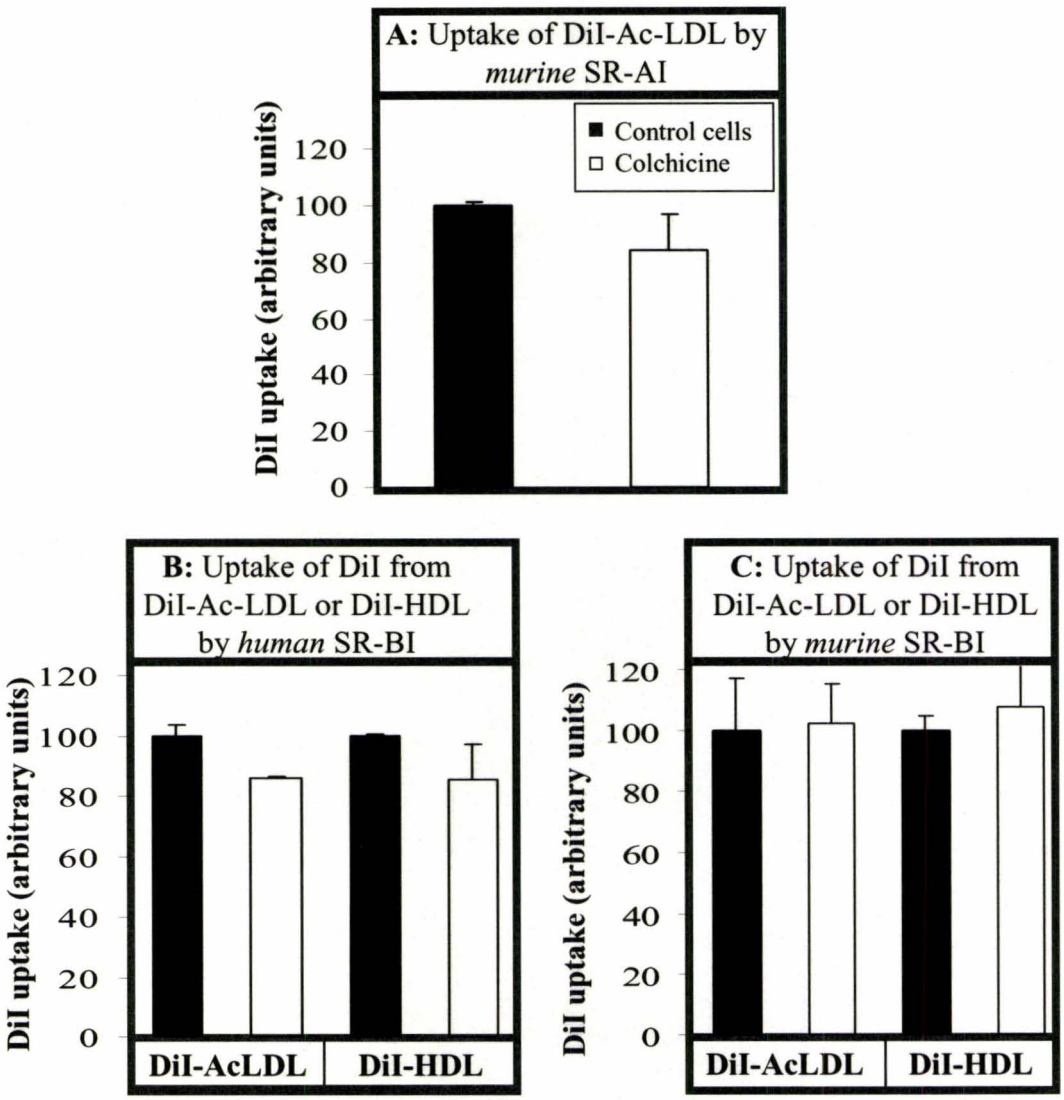

Figure 21: Effect of colchicine on uptake of DiI from DiI-Ac-LDL or DiI-HDL by human and murine SR-BI. Control CHO[*murine* SR-AI] (panel A), ldlA[*human* SR-BI] (panel B) or ldlA[*murine* SR-BI] (panel C) cells were cultured in media containing 3 % NCLPDS for two days. On day three, control cells were treated with (open bars) or without (solid bars) 10 μM colchicine in media containing 0.5 % BSA for 2 hrs prior to and during incubation with DiI-Ac-LDL or DiI-HDL (each 5 μg/ml) at 37°C and subsequent flow cytometric analysis as described in section (*as described in section 2.2.12.2*) Average DiI uptake values are expressed relative to control levels (set at 100).

Taken together, data from flow cytometric analysis and live fluorescence microscopy suggests that disruption of microtubules does not significantly affect DiI uptake from lipoproteins, but it does have an effect on trafficking of the fluorescent lipid once it has been internalized. The results of these experiments also establish that the inhibitory effect of cytochalasin D on SR-BI mediated DiI uptake was a specifically due to disrupting microfilament function and not an artifact of disrupting the cytoskeletal structure of cells.

4. Discussion

SR-BI is an interesting receptor, as its broad binding specificity allows it to interact with a variety of different ligands. Like most scavenger receptors, SR-BI can bind modified lipoproteins. However, while other scavenger receptors such as SR-AI mediate the endocytic internalization leading to lysosomal hydrolysis of the entire lipoprotein particle (Brown et al., 1979), SR-BI appears to be unique in its ability to selectively transfer lipid components of unmodified lipoprotein particle into the cell (Acton et al., 1994; Krieger, 2001; Silver et al., 2001[a]). This process of *selective uptake* of lipids without the *net* internalization of the lipoprotein has been investigated by several groups of scientists for HDL. It has been shown that HDL particles appear to be transiently internalized by cells (Silver et al., 2001[b]). There is also evidence to support that SR-BI is active in lipid uptake from HDL when reconstituted in liposomes in the absence of other cellular machinery (Liu and Krieger, 2002). However, to date the mechanisms involved in SR-BI mediated transfer of lipid from HDL and other lipoproteins have not been fully characterized. We set out to investigate whether SR-BI mediated endocytosis of lipoprotein particles plays a role in SR-BI mediated lipid transfer from lipoproteins. We have investigated the effect of blocking different steps in endocytosis on the uptake of lipid from lipoproteins in cells.

SR-BI appears to have distinct binding sites for different ligands including HDL and Ac-LDL. We therefore explored whether SR-BI mediated lipid uptake from distinct lipoprotein ligands may involve distinct mechanisms. We used HDL and Ac-LDL as ligands for these studies for two reasons *1)* the ease of incorporating the fluorescent lipid

DiI into these lipoproteins and *2)* they have been shown to bind to the receptor via distinct sites (Gu et al., 2000; Gu et al., 2000[a]). DiI labeling of lipoproteins is often used to track the transfer of lipid from lipoprotein particles (Acton et al., 1996; Silver et al., 2001[b]). and has previously been shown to be a reliable marker of SR-BI mediated cholesterol ester transfer from lipoproteins to cells (Acton et al., 1996).

In order to study SR-BI mediated lipid uptake we used model cell lines *1)* ldlA7 cells, a CHO cell line that lacks a functional LDL receptor; *2)* ldlA[*murine* SR-BI] cells, derivatives of ldlA7 stably expressing *murine* SR-BI (established by M. Kreiger (Acton et al., 1996). We also established cell lines expressing *human* SR-BI, ldlA[*human* SR-BI] and recombinant *human* SR-BI with either EGFP or mRFP fused to its amino terminus, ldlA[EGFP-*human*-SR-BI] or ldlA[mRFP-*human*-SR-BI].

Murine SR-BI and *human* SR-BI share 80% sequence identity (Calvo et al., 1995; Calvo et al., 1997). *Human* SR-BI (also referred to as the "CD36 like antigen-1", or CLA-1) binds HDL with a dissociation constant reported to be 35 μg/ml, (Calvo et al., 1997) similar to 30 μg/ml reported for *murine* SR-BI (Acton et al., 1996). Like *murine* SR-BI, *human* SR-BI was also shown to exhibit selective uptake of lipid from HDL (Calvo et al., 1997; Murao et al., 1997). *Human* SR-BI was shown to be a high-affinity specific receptor for the lipoproteins HDL, LDL, VLDL, OxLDL, and AcLDL (Calvo et al., 1997; Murao et al., 1997) as well as native LDL and anionic phospholipids (Calvo et al., 1997) like previously shown for *murine* SR-BI. Finally, *human* SR-BI was shown to be expressed abundantly in the adrenal gland, liver and testis (Calvo et al., 1995),

suggesting that *human* SR-BI, like *murine* SR-BI, could play a role in the metabolism of HDL (Calvo et al., 1997; Murao et al., 1997).

In addition to testing the role of endocytosis on SR-BI mediated DiI uptake in stable cell lines expressing untagged *murine* and *human* SR-BI, we used EGFP- or mRFP labeled *human* SR-BI to study the sub-cellular localization, and interaction of SR-BI with components of endocytic pathway (clathrin) as well as the dynamics of SR-BI mediated DiI transfer from lipoproteins.

4.1. SR-BI mediated lipid uptake is sensitive to treatments inhibiting endocytosis in cells

Initially, we used treatments, like potassium depletion and incubation of cells stably expressing *murine* SR-BI and *human* SR-BI with a hyperosmolar sucrose concentration, to study the effect of inhibiting receptor mediated endocytosis on SR-BI mediated transfer of lipid from lipoproteins. These treatments have been shown to block clathrin mediated endocytosis by interfering with clathrin assembly and the formation of functional clathrin coated pits (Heuser and RG, 1989; Larkin et al., 1983). The exact mechanism by which these treatments block caveolae mediated endocytosis in not known, but these treatments have shown to result in a decrease in cell surface caveolae and to inhibit the uptake of mediated uptake of markers of caveolae mediated uptake (Carpentier et al., 1989). It is possible that these treatments may affect a common step(s) to a variety of different endocytic pathways.

In potassium depleted cells, there was an inhibition of *human* SR-BI mediated DiI uptake from DiI-Ac-LDL and DiI-HDL by 72 % and 70% respectively, whereas *murine* SR-BI mediated DiI uptake from DiI-Ac-LDL was inhibited by 66%. These differences were statistically significant versus control cells ($p < 0.023$). In contrast, there was only a 30% decrease in DiI uptake from DiI-HDL by *murine* SR-BI (not statistically significant, $p= 0.1$). Similar results were seen when cells were treated with hyperosmotic sucrose concentrations. DiI uptake from DiI-Ac-LDL and DiI-HDL by *human* SR-BI was inhibited by 83 % and 61% respectively, while DiI uptake from DiI-Ac-LDL by *murine* SR-BI was decreased by 70 % ($p<0.032$). In contrast, DiI uptake from DiI-HDL by *murine* SR-BI was decreased by only 20% (not statistically significant, $p = 0.51$). This suggests that the mechanism of *murine* SR-BI mediated DiI-uptake from Ac-LDL but not HDL is dependent on cellular endocytosis.

4.2. SR-BI mediated lipid transfer requires intact microfilaments and microtubules

Microtubules are long filamentous structures that are important in organellar localization, as well as transport of cargo between organelles. Movement along microtubules is relatively rapid (~1 μm/s) and can occur over long distances (Apodaca, 2001). Microfilaments (actin filaments) have also been implicated in the localization of intracellular organelles and vesicular transport. Unlike microtubules, actin filaments are generally shorter and actin based transport is much slower (~ 0.1 μm/s) (Apodaca, 2001). Microfilaments have been shown to be involved in the internalization step of receptor

mediated endocytosis; in clathrin mediated uptake of ligands (Durrbach et al., 1996; Osland et al., 1979) as well as as the internalization of caveolae (RG Parton, 1994).

To evaluate the involvement of microfilaments and microtubules in SR-BI mediated lipid uptake, we tested the effect of disrupting these structures in cells, using cytochalasin D and colchicine, on *human* and *murine* SR-BI mediated lipid uptake. Cytochalasin D is commonly used to disrupt microfilament-dependent processes because it inhibits actin cross linking and polymerization (Goddette and Frieden, 1986; Cooper, 1987). Cytochalasin D treatment resulted in a 34 and 60% decrease in *human* SR-BI mediated DiI uptake from DiI-HDL and DiI-Ac-LDL, respectively. There was a 54% decrease in *murine* SR-BI mediated DiI uptake from DiI-Ac-LDL. These were comparable to the 51% decrease in DiI-Ac-LDL uptake by control SR-AI expressing cells. In contrast there was no significant decrease in *murine* SR-BI mediated lipid uptake from DiI-HDL. Our results suggest that microfilaments play an important role in *human* SR-BI mediated DiI uptake from DiI-HDL and DiI-Ac-LDL and in *murine* DiI uptake from DiI-Ac-LDL. This result is similar to the results obtained from potassium depletion and hyperosmolarity. Disruption of microtubules, on the other hand, did not affect DiI uptake in cells regardless of the receptor or ligand, suggesting that microtubules do not have a role in SR-BI mediated lipid uptake from lipoproteins.

Live cell imaging of the cells expressing EGFP-*human*-SR-BI after incubation with DiI labelled lipoproteins showed that DiI lipid and *human* SR-BI are present in dynamic vesicles in the cells. DiI and *human* SR-BI co-localize (partially) in these dynamic vesicles as well as on the cell periphery, especially at the areas of cell- cell

contact. Co-localization of SR-BI and DiI in dynamic vesicles may suggest vesicular trafficking of *human* SR-BI and DiI lipid within the same compartments. Vesicles containing DiI, EGFP-*human*-SR-BI or both are generally spherical, have different sizes relative to each other, and display a variety of motions in the cell. There is rapid movement covering long distances, as well as localized short range movements. These vesicles travel in three dimensions, indicated by their movement in an out of the focal plane as well as along the focal plane of observation, during microscopy. Movement of these vesicles are similar to those mediated by microtubules and microfilament earlier; although more quantitative analysis (e.g. measuring the rate of movement of vesicles) would have to be done to qualify their motion as microtubular or actin dependent.

Although the total uptake of DiI was not affected by colchicine, images of live adherent cells (expressing untagged *murine* or *human* SR-BI) treated with cholchicine revealed that colchicine completely stopped the movement of DiI containing vesicles in cells. As microtubules are shown to be involved in the movement of cargo within endocytic compartments (Goddette and Frieden, 1986; Osland et al., 1979), these results suggest a role of microtubules in trafficking of lipoprotein derived lipid in cells, but not in the uptake of lipid by *human* and *murine* SR-BI.

It is interesting to note that live cell imaging of cells EGFP-*human*-SR-BI revealed that in the presence of cytochalasin D, there was an increased in DiI and SR-BI co-localization on what appeared to be near or on the cell membrane. It appears that DiI fluorescence is concentrated in endocytic vesicles containing EGFP-*human*-SR-BI, on or near the surface of plasma membrane. This observation is consistent with the role of

microfilament in internalization of endocytic vesicles, and reduced total DiI uptake from lipoproteins. Due to the inability of cells to internalize these vesicles, the total uptake of DiI from lipoprotein is reduced.

4.3. SR-BI mediated lipid uptake appears not to involve clathrin

Previous research has demonstrated that *murine* SR-BI partially co-localized with caveolin-1 in a low density subfraction of plasma membranes in a number of cell types including CHO cells (Babitt et al., 1997). That study showed that SR-BI did not co-localize with clathrin (Babitt et al., 1997). However those experiments were done in the absence of added lipoproteins. SR-AI has been shown to mediate endocytic uptake of Ac-LDL via clathrin coated pits. The results of potassium depletion and hypertonic treatment described above, demonstrate that *human* SR-BI-mediated DiI Ac-LDL and HDL uptake behaved in a manner similar to SR-AI-mediated DiI-Ac-LDL uptake. We therefore decided to test whether *human* SR-AI co-localized with clathrin. We showed in Figure 8 that the overall distribution of EGFP-tagged and mRFP-tagged *human* SR-BI was similar to that previously described for *murine* SR-BI.

We used cells stably expressing mRFP-*human*-SR-BI and EGFP-Clathrin (light chain) to study the co-localization in the absence or presence of either Ac-LDL or HDL. Our results showed that the two proteins do not co-localize in cells, even in the presence of ligands. These results suggest that SR-BI mediated uptake of lipids from lipoproteins does not involve clathrin mediated endocytosis. However, one caveat is that these studies were performed on fixed cells; it remains possible that fixation may have altered the

distribution of these proteins. Live cell imaging should therefore be performed to ensure that there is no interaction between the two proteins in the presence and absence of lipoproteins.

Co-localization studies using yellow fluorescence tagged wild type caveolin 1 or DiI uptake in cells expressing mutant caveolins (constitutively active (S80E) or inactive (S80A) (Schlegel et al., 2001), generated by fusion of yellow fluorescent protein on the c-terminus of Caveolin, not discussed in the thesis) can be used to establish the role of caveolae mediated endocytosis in SR-BI mediated lipid transfer by SR-BI.

4.4. SR-BI mediated lipid uptake from lipoproteins is dynamin dependent

Dynamin dependence is the hallmark of several endocytic pathways in cells, including clathrin mediated and caveolae mediated endocytosis (Fisha et al., 2000; Henley et al., 1998). The dynamin family of GTPase's are involved in the fission of clathrin coated pits from the cell membrane and the formation of clathrin coated vesicles, a rate determining step in clathrin coated pit mediated internalization (Sever et al., 2000). Dynamin is also involved in pinching of caveolae from the cell membrane, and its subsequent internalization (Henley et al., 1998).

Dynamin-dynamin interactions are critical in regulating its cellular function. It has been shown that self-assembly of dynamins (into heteromers) increases GTPase activity (Muhlberg et al., 1997), which is critical for its function. Dyn1-K44A, a dominant-negative mutant form of dynamin 1 has been shown to block receptor mediated endocytosis, due to its impaired GTP binding and hydrolysis (Damke et al., 2001). We

used a hemagluttinin epitope tagged version of Dyn1-K44A (HA-Dyn1-K44A) to study the dynamin dependence of *human* and *murine* SR-BI mediated lipid uptake from DiI-Ac-LDL and DiI-HDL. Our results indicated that both *murine* SR-BI as well as *human* SR-BI mediated lipid transfer from both lipoprotein ligands is inhibited by 30 percent (*refer to table 2*). A 30% inhibition in DiI uptake is modest compared to the inhibition due to potassium depletion and hyperosmotic incubation conditions. It is important to point out that DiI uptake in control CHO [*murine* SR-AI] cells (known to take up DiI-Ac-LDL via clathrin mediated endocytosis) was affected to the same degree. Moreover, HA-Dyn1-K44A mediated inhibition of DiI uptake was statistically significant ($p < 0.002$). Our data suggests that *human* and *murine* SR-BI mediated lipid uptake from Ac-LDL and HDL is dynamin dependent.

Table2: Effect of Dyn1-K44A expression on DiI uptake from DiIAcLDL and DiIHDL, by *human* and *murine* SR-BI.

Cell line	Lipoprotein Ligands	% Inhibition of DiI uptake*
Murine SR-AI	DiIAcLDL	29%
Murine SR-BI	DiIAcLDL	28%
Murine SR-BI	DiIHDL	30%
Human SR-BI	DiIAcLDL	37%
Human SR-BI	DiIHDL	36%

* $p < 0.002$

4.5. Summary and Conclusion

The goal of our study was to assess the role of endocytosis in SR-BI mediated lipid uptake from lipoproteins. Our focus tended to be on caveolae and clathrin dependent endocytosis, as those are the two best characterized endocytic pathways in cells. Our investigation showed a few interesting and novel aspects of SR-BI mediated lipid uptake. We have shown that *human* SR-BI appears to take up lipoproteins from both modified and unmodified lipoproteins in an actin, dynamin and endocytosis dependent manner, suggesting that endocytosis plays a role in this process. In contrast, *murine* SR-BI appears to mediate lipid uptake from modified lipoproteins and unmodified lipoproteins in a differential manner. Lipid uptake from modified lipoproteins is dependent on endocytosis, while lipid uptake from unmodified lipoproteins is not. However, dynamin dependence of SR-BI mediated lipid uptake from both ligands suggests that HDL might still be internalized in a receptor dependent manner, albeit via a lesser known or specialized endocytic mechanism, which is not sensitive to potassium depletion, hyperosmolarity, or actin depolymerization. We showed that although microtubules are not essential for SR-BI mediated lipid uptake, they are important in the trafficking of lipoprotein derived lipid in the cells.

In the light of our finding that SR-BI mediated lipid uptake by human SR-BI differs from that of murine SR-BI. We took a closer look at the amino acid sequence of *human* and *murine* SR-BI and noticed a curious difference. We found that *human* SR-BI contains a four amino acid long tyrosine based putative internalization signaling sequence YLΦW, in the carboxyl terminal cytoplasmic region, which could potentially be a

tyrosine dependent AP-2 recognition and binding site (YXXΦ) (Hinshaw, 2000; Nesterov et al., 1999). In *murine* SR-BI the tyrosine (Y) is replaced with a phenylalanine (F). Figure 22 below, shows that the four amino acid sequence is conserved in pigs, bovines, humans and rabbits; however, it is not conserved in mice, rats and Chinese hamsters.

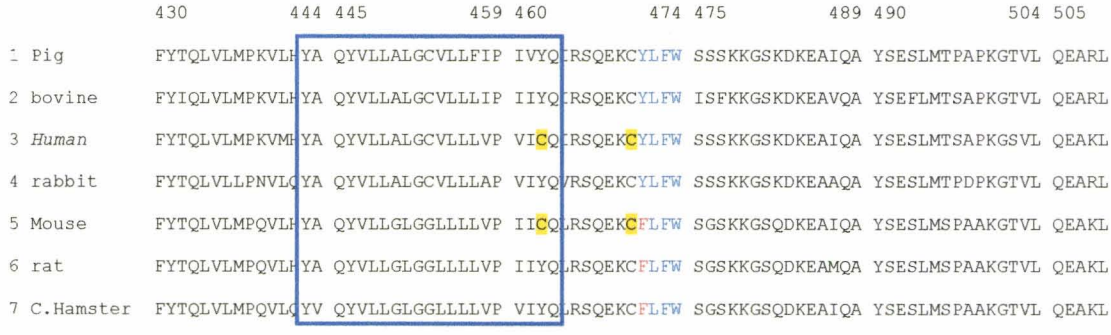

Figure 22. Figure shows an Alignment of the the carboxyl terminal region of SR-BI in pig, bovine, human rabbit, mouse, rat and Chinese hamster. The proposed transmembrane sequence is enclosed in the blue rectangle. Putative AP-2 binding site is highlighted in blue. Palmitoylation at cysteine residues 462 and 470 are highlighted.

Investigating the role of this putative signal sequence might provide insight into the difference between the mechanism of *human* and *murine* SR-BI mediated lipid uptake from HDL.

5. References

Acton, S., Rigotti, A., Landschulz, K., Xu, S., Hobbs, H., and Krieger, M. 1996. Identification of Scavenger Receptor LDL as a High Density Lipoprotein Receptor. *Science*. 271:518-20.

Acton, S.L., Scherer, P.E., Lodish, H.F., and Krieger, M. 1994. Expression Cloning of SR-BI, a CD36 Class B Receptor. *Journal of Biological Chemistry*. 269:21003-21009.

Altschuler, Y.S., Barbas, M., Terlecky, L.J., Tang, S.K., and L., S.S. 1998. Redundant and Distinct Functions for Dynamin-1 and Dynamin-2 Isoforms. *Journal of Cell Biology*. 143:1871-1881.

Anderson, R.G., Kamen, B.A., Rothberg, K.G., and S.W, L. 1992. Potocytosis: Sequestration and Transport of Small Molecules by Caveolae. *Science*. 255:410-1.

Apodaca, G. 2001. Endocytic Traffic in Polarized Epithelial Cells: Role of the Actin and Microtubule Cytoskeleton. *Traffic*. 2:149-159.

Babitt, J., Trigatti, B., Rigotti, A., Smart, E.J., Anderson, R.G.W., Xu, S., and Krieger, M. 1997. Murine SR-BI, a High Density Lipoprotein Receptor That Mediates Selective Lipid Uptake, Is N-Glycosylated and Fatty Acylated and Colocalizes with Plasma Membrane Caveolae. *Journal of Biological Chemistry*. 272:13242-13249.

Beglova. 2004. Cooperation between Fixed and Low pH-Inducible Interfaces Controls Lipoprotein Release by the LDL Receptor. *Molecular Cell*. 16:281- 292.

Brown, M.S., and Goldstein, J.L. 1986. A Receptor-Mediated Pathway for Cholesterol Homeostasis. *Science*. 232:33-47.

Brown, M.S., Ho, Y.K., and Goldstein, J.L. 1979. Binding Sites on Macrophages That Mediates Uptake and Degradation of Acetylated Low Density Lipoprotein Produces Massive Cholesterol Deposition. *Proceedings of National Academy of Science USA*. 76:333-337.

Calvo, D., Dopazo, J., and Vega, M.A. 1995. The CD36, CLA-1 (CD36L1), and LIMPII(CD36L2) Gene Family: Cellular Distribution, Chromosomal Location, and Genetic Evolution. *Genomics*. 25:100-6.

Calvo, D., Gomez-Coronado, D., Lasuncion, M.A., and Vega, M.A. 1997. CLA-1 Is an 85-KD Plasma Membrane Glycoprotein That Acts as a High-Affinity Receptor for Both Native (HDL, LDL, and VLDL) and Modified (OxLDL and AcLDL) Lipoproteins. *Arteriosclerosis, Thrombosis and Vascular Biology*. 11:2341-9.

Calvo, D., and Vega, M.A. 1993. Identification, Primary Structure, and Distribution of CLA-1, Novel Member of the CD36/LimpII Gene Family. *Journal of Biological Chemistry*. 268:18929-18935.

Cardelli, J. 2001. Phagocytosis and Macropinocytosis in Dictyostelium: Phosphoinositide Based Processes, Biochemically Distinct. *Traffic*. 2:311-320.

Carpentier, J.L., Sawano, F., Geiger, D., Gorden, P., Perrelet, A., and Orci, L. 1989. Potassium Depletion and Hypertonic Medium Reduce "Non-Coated" and Clathrin-Coated Pit Formation, as Well as Endocytosis through These Two Gates. *Journal of Cell Physiology*. 138:519-26.

Cooper, J.A. 1987. Effects of Cytochalasin and Phalloidin on Actin. *Journal of Cell Biology*. 105:1473-1478.

Covey, S.D., Krieger, M., Wang, W., Penman, M., and Trigatti, B.L. 2003. Scavenger Receptor Class B Type I-Mediated Protection against Atherosclerosis in LDL Receptor-Negative Mice Involves Its Expression in Bone Marrow-Derived Cells. *Arteriosclerosis Thrombosis, and Vascular Biology*. 23:1589-1594.

Damke, H., Binns, D.D., Ueda, H., Schmid, S.L., and Baba, T. 2001. Dynamin GTPase Domain Mutants Block Endocytic Vesicle Formation at Morphologically Distinct Stages. *Molecular Biology of the Cell*. 12:2578-2589.

Daukas, G., and Zigmond, S.H. 1985. Inhibition of Receptor-Mediated but Not Fluid-Phase Endocytosis in Polymorphonuclear Leukocytes. *Journal of Cell Biology*. 101:1673-1679.

de Villiers, W.J., and Smart, E.J. 1999. Macrophage Scavenger Receptors and Foam Cell Formation. *Journal of Leukocyte Biology*. 66:740-6.

de Winther, M.P.J., Van, D.K.W., Havekes, L.M., and Hofker, M.H. 1999. Macrophage Scavenger Receptor Class A. A Multifunctional Receptor in Atherosclerosis. *Arteriosclerosis, Thrombosis and Vascular Biology*:291-297.

Durrbach, A., Louvard, D., and Coudrier, E. 1996. Actin Filaments Facilitate Two Steps of Endocytosis. *Journal of Cell Science*. 109:457-465.

Fisha, K.N., Schmid, S.L., and Hanna, D. 2000. Evidence That Dynamin-2 Functions as a Signal-Transducing GTPase. *Journal of Cell Biology*. 150:145-154.

Fujimoto, L., Miya, R., Heuser, J.E., and Schmid, S.L. 2000. Actin Assembly Plays a Variable, but Not Obligatory Role in Receptor-Mediated Endocytosis. *Traffic*. 1:161-171.

Gilbert, A., Paccaud, J.P., Foti, M., Porcheron, G., Balz, J., and Carpentier, J.L. 1999. Direct Demonstration of the Endocytic Function of Caveolae by a Cell-Free Assay. *Journal of Cell Science*. 112:1101-1110.

Goddette, D.W., and Frieden, C. 1986. Actin Polymerization. The Mechanism of Action of Cytochalasin D. *Journal of Biological Chemistry*. 261:15974-80.

Gu, X., Kozarsky, K., and Kreiger, M. 2000. Scavenger Receptor Class B Type I Mediated [^{3}H] Cholesterol Efflux to High Density and Low Density Lipoprotein Binding to the Receptor. *Journal of Biological Chemistry*. 275:29993-30001.

Gu, X., Lawrance, R., and Kreiger, M. 2000[a]. Dissociation of the High Density Lipoprotein Binding Activity of Murine Scavenger Receptor Class B Type One, Using Reterovirus Library Based Activity Dissection. *Journal of Biological Chemistry*. 275:9120-9130.

Henley, J.R., Krueger, E.W.A., Oswald, B.J., and McNiven, M.A. 1998. Dynamin-Mediated Internalization of Caveolae. *Journal of Cell Biology*. 141:85-99.

Heuser, J., and Anderson R.G. 1989. Hypertonic Media Inhibit Receptor-Mediated Endocytosis by Blocking Clathrin-Coated Pit Formation. *Journal of Cell Biology*. 108:389-400.

Hinshaw, J.E. 2000. Dynamin and Its Role in Membrne Fission. *Annual Review of Cell and Developmental Biology*. 16:483-519.

Howell, J.L., and Truant, R. 2002. Live-Cell Nucleocytoplasmic Protein Shuttle Assay Utilizing Laser Confocal Microscopy and FRAP. *Biotechniques*. 232:80-2, 84, 86-7.

Iacopetta, B.J., and Morgan, E.H. 1983. The Kinetics of Transferrin Endocytosis and Iron Uptake from Transferrin in Rabbit Reticulocytes. *Journal of Biological Chemistry*. 258:9108-15.

Ikemoto, M., Arai, H., Feng, D., Tanaka, K., Aoki, J., Dohmae, N., akio, K., Adachi, H., Tsujimoto, M., and Inoue, K. 2002. Identification of a PDZ-Domain-Containing

Protein That Interacts with the Scavenger Receptor Class B Type I. *Proceedings of National Academy of Science USA*. 97:6538-6543.

Janet, M. 1983. Depletion of Intracellular Potassium Arrests Coated Pit Formation and Receptor Mediated Endocytosis in Fibroblasts. *Cell*. 33:273-285.

Kirchhausen, T., and Harrison, S.C. 1981. Protein Organization in Clathrin Trimers. *Cell*. 23:755-761.

Kodama, T., and Freeman, M. 1990. Type I Macrophage Scavenger Receptor Contains Alpha-Helics and Collegen Like Coiled-Coils. *Nature*. 343:531-535.

Kozarsky, K.F., Donahee, M.H., Rigotti, A.I., Iqbal, S.N., Edelman, E.R., and Krieger, M. 1997. Overexpression of the HDL Receptor SR-BI Alters Plasma HDL and Bile Cholesterol Levels. *Nature*. 387:414-7.

Krieger, M. 2001. Scavenger Receptor Class B I Is a Multiligand HDL Receptor That Influences Diverse Physiological Systems. *Journal of Clinical Investigation*. 108:793-7.

Krieger, M., and Herz, J. 1994. Structures and Functions of Multiligand Lipoprotein Receptors: Macrophage Scavenger Receptors and LDL Receptor-Related Protein (LRP). *Annual Review of Biochemistry*. 63:601-637.

Laemmli, U. 1970. Cleavage of Structural Proteins During the Assembly of the Head of Bacteriophage T4. *Nature*. 227:680-5.

Larkin, J.M., Brown, M.S., J.L, G., and Anderson, R.G. 1983. Depletion of Intracellular Potassium Arrests Coated Pit Formation and Receptor-Mediated Endocytosis in Fibroblasts. *Cell*. 33:273-85.

Liu, B., and Krieger, M. 2002. Highly Purified Scavenger Receptor Class B, Type I Reconstituted into Phosphatidylcholine/Cholesterol Liposomes Mediates High Affinity High Density Lipoprotein Binding and Selective Lipid Uptake. *Journal of Biological Chemistry*. 277:34125-34135.

Marsche, G., Hammer, A., Oskolkova, O., Kozarsky, K.F., Sattler, W., and Malle, E. 2002. Hypochlorite-Modified High Density Lipoprotein, a High Affinity Ligand to Scavenger Receptor Class B, Type I, Impairs High Density Lipoprotein-Dependent Selective Lipid Uptake and Reverse Cholesterol Transport. *Journal of Biological Chemistry*. 277:32172-32179.

Matveev, S., Uittenbogaard, A., van der Westhuyzen, D., and Smart, E.J. 2001. Caveolin-1 Negatively Regulates SR-BI Mediated Selective Uptake of High-Density

Lipoprotein-Derived Cholesteryl Ester. *European Journal of Biochemistry.* 268:5609-5616.

Mueller, V.J., Wienisch, M., Nehring, R.B., and Klingauf, J. 2004. Monitoring Clathrin-Mediated Endocytosis During Synaptic Activity. *Journal of Neuroscience.* 24:2004-2012.

Muhlberg, A.B., Warnock, D.E., and Schmid, S.L. 1997. Domain Structure and Intramolecular Regulation of Dynamin GTPase. *EMBO Journal.* 16:6676-6683.

Mundy D I. , M.T., Ying Yun-shu, Anderson Richard G.W. and Bloom George S. 2002. Dual Control of Caveolar Membrane Traffic by Microtubules and the Actin Cytoskeleton. *Journal of Cell Science.* 115:1-13.

Murao, K., Terpstra, V., Green, S.R., Kondratenko, N., Steinberg, D., and Quehenberger, O. 1997. Characterization of Cla-1, a Human Homologue of Rodent Scavenger Receptor BI, as a Receptor for High Density Lipoprotein and Apoptotic Thymocytes. *Journal of Biological Chemistry.* 272:17551-17557.

Nabi, I.R., and Le, P.U. 2003. Caveolae/Raft-Dependent Endocytosis. *Journal of Cell Biology.* 161:673-677.

Nesterov, A., Carter, R.E., and T, S. 1999. Inhibition of the Receptor-Binding Function of Clathrin Adaptor Protein AP-2 by Dominant-Negative Mutant 2 Subunit and Its Effects on Endocytosis. *EMBO Journal.* 18:2489-2499.

Nichols, B. 2003. Caveosomes and Endocytosis of Lipid Rafts. *Journal of Cell Science.* 116:4707-4714.

Oh, P., McIntosh, D.P., and Schnitzer, J.E. 1998. Dynamin at the Neck of Caveolae Mediates Their Budding to Form Transport Vesicles by GTP-Driven Fission from the Plasma Membrane of Endothelium. *Journal of Cell Biology.* 141:101-114.

Ohgami, N., NagaiI, R., Ikemoto, M., Arai, H., Kuniyasu, A., Horiuchi, S., and Nakayamaa, H. 2001. CD36, a Member of Class B Scavenger Receptor Family, Is a Receptor for Advanced Glycation End Products. *Annals of the New York Academy of Sciences.* 947:350-355.

Osland, R.E., Pfleger, B., and Schonfeld, G. 1979. Role of Microtubules in Low Density Lipoprotein Processing by Cultured Cells. *Journal of Clinical Investigation.* 63:75-84.

Pelkmans, L., and Helenius, A. 2002. Endocytosis Via Caveolae. *Traffic.* 3:311-320.

Qualmann, B., Kessels, M.M., and Kelly, R.B. 2000. Molecular Links between Endocytosis and the Actin Cytoskeleton. *Journal of Cell Biology*. 150:F111–F116.

Parton, R.G., Joggerst, B., and Simons, K. 1994. Regulated Internalization of Caveolae. *Journal of Cell Biology*. 127:1199-1215.

Ricotta, D., Conner, S., Schmid, S., von Figura, and Honing, S. 2002. Phosphorylation of the AP2 Mu Subunit by Aak1 Mediates High Affinity Binding to Membrane Protein Sorting Signals. *Journal of Cell Biology*. 156:791-5.

Rigotti, A., Acton, S.L., and Krieger, M. 1995. The Class B Scavenger Receptors SR-BI and CD36 Are Receptors for Anionic Phospholipids. *Journal of Biological Chemistry*. 270:16221-16224.

Rigotti, A., Trigatti, B.L., Penman, M., Rayburn, H., Herz, J., and Krieger, M. 1997. A Targeted Mutation in the Murine Gene Encoding the High Density Lipoprotein (HDL) Receptor Scavenger Receptor Class B Type I Reveals Its Key Role in HDL Metabolism. *Proceedings of National Academy of Science USA*. 94:12610-12615.

Rodrigueza, W.V., Thuahnai, S.T., Temel, R.E., Lund-Katz, S., Phillips, M.C., and William, D.L. 1999. Mechanism of Scavenger Receptor Class B Type I-Mediated Selective Uptake of Cholesteryl Esters from High Density Lipoprotein to Adrenal Cells. *Journal of Biological Chemistry*. 274:20344-20350.

Schlegel, A., Arvan, P., and Lisanti, M.P. 2001. Caveolin-1 Binding to Endoplasmic Reticulum Membranes and Entry into the Regulated Secretory Pathway Are Regulated by Serine Phosphorylation. Protein Sorting at the Level of the Endoplasmic Reticulum. *Journal of Biological Chemistry*. 276:4398-4408.

Sever, S., Damke, H., and Schmid, S.L. 2000. Dynamin:GTP Controls the Formation of Constricted Coated Pits, the Rate Limiting Step in Clathrin-Mediated Endocytosis. *Journal of Cell Biology*. 150:1137-1148.

Silver, D.L., Nan, W., Xio, X., and Tall, A.R. 2001[b]. HDL Particle Uptake Mediated by SR-BI Results in Selective Sorting of HDL Cholesterol from Protein and Polarized Secretion. *Journal of Biochemistry*. 276:25287-25293.

Silver, D.L., and Tall, A.R. 2001[a]. Cell Biology of SR-BI. *Current Opinion in Lipidology*. 12:497- 504.

Stangl, H., Hyatt, M., and Hobbs, H.H. 1999. Transport of Lipids from High and Low Density Lipoproteins Via Scavenger Receptor-BI. *Journal of Biological Chemistry*. 274:32692-32698.

Subtil, A., Hemar, A., and Dautry-Varsat, A. 1994. Rapid Endocytosis of Interleukin 2 Receptors When Clathrin-Coated Pit Endocytosis Is Inhibited. *Journal of Cell Science*. 107:3461-3468.

Swansona, J.A., and Watts, C. 1995. Macropinocytosis. *Trends in Cell Biology*. 5:11

Trigatti, B.L., Rigotti, A., and Braun, A. 2000. Cellular and Physiological Roles of SR-BI, a Lipoprotein Receptor Which Mediates Selective Lipid Uptake. *Biochimica et Biophysica Acta*.1529:276-286.

Ungewickell, E., and Branton, D. 1981. Assembly Units of Clathrin Coats. Assembly Units of Clathrin Coats. *Nature*. 289:420-422.